Palacký University Olomouc

Bachelor Thesis

Olomouc 2021 **Kamila Baslarová**

Palacký University Olomouc

Faculty of Science

Department of Cell Biology and Genetics

Lipidomic Analysis of Exhaled Breath Condensate

Bachelor Thesis

Kamila Baslarová

Study programme: Biology

Field of study: Molecular and cell biology

Form of study: Full time

Olomouc 2020 **Supervisor: prof. Juan Bautista de Sanctis PhD.**

UNIVERZITA PALACKÉHO V OLOMOUCI

Přírodovědecká fakulta

Akademický rok: 2019/2020

ZADÁNÍ BAKALÁŘSKÉ PRÁCE

(projektu, uměleckého díla, uměleckého výkonu)

Jméno a příjmení:	**Kamila BASLAROVÁ**
Osobní číslo:	**R18637**
Studijní program:	**B1501 Biologie**
Studijní obor:	**Molekulární a buněčná biologie**
Téma práce:	**Analýza lipidů v dechovém kondenzátu**
Zadávající katedra:	**Katedra buněčné biologie a genetiky**

Zásady pro vypracování

LIPIDOMIC ANALYSIS OF EXHALED BREATH CONDENSATE (EBC)

Bronchoscopy and bronchoalveolar lavage are conventional, precise, and invasive methods used to examine lung function. Exhaled breath condensate (EBC) is a simple, non-invasive method that can provide useful information about lung function. The air exhaled from the lower respiratory tract is collected by tubing and condensated at low temperatures. The obtained aqueous solution contains several biomarkers: volatile gases and non-volatile compounds like fatty acids, ceramides, eicosanoids and peptides, and proteins (cytokines). Ceramides are metabolites derived from the enzymatic modification of fatty acids and sphingosine. They are a structural component of lipid membranes and signalling molecules capable of inducing apoptosis, moderating cell proliferation and differentiation. Increased levels of sphingolipids and ceramides are recorded in the plasma of patients with asthma, in cell cultures exposed to cigarette smoke, and in some phenotypes of chronic obstructive pulmonary disease. The assessment of ceramides has not been performed in EBC samples. The thesis aims to standardize a method to analyze and quantitate ceramides in the EBC of healthy volunteers.

Materials and methods. EBC will be collected from at least 20 healthy, normal spirometry, non-smokers ages 20-23. To obtain the samples, volunteers will exhale into collecting tube for 10 minutes. EBC will be collected by condensation at a temperature –5 °C. Sin order to avoid saliva contamination, the tubing will contain saliva traps. Lipids will be extracted from EBC by a mixture of methanol and chloroform (1:2 v/v) Folch method. Then, the samples will be dried and resuspended in methanol to analyze them by HPLC-MS. The PUFA will be quantified according to a standard curve. We will try to study, in the same sample, the amount of ergosterol. Ergosterol will be used as a biomarker for the presence of a fungal pathogen, *Aspergillus* spp, which is responsible for inflammation of the sinus and upper airways.

Expected results: we expect to detect and quantitate ceramides in EBC of normal controls and correlate the values with pathogens' presence.

1. SPHINGOLIPIDS

1.1 CERAMIDES

1.2 SHINGOLIPIDS AND CERAMIDES WITHIN LUNGS DISEASE

3. MASS SPECTROFOTOMETRY

4.CHLOROFORM-METHANOL EXTRACTION

Rozsah pracovní zprávy:	
Rozsah grafických prací:	
Forma zpracování bakalářské práce:	**tištěná**
Jazyk zpracování:	**Angličtina**

Seznam doporučené literatury:

MUTLU, GÖKHAN M., KEVIN W. GAREY, RICHARD A. ROBBINS, LARRY H. DANZIGER a ISRAEL RUBINSTEIN. Collection and Analysis of Exhaled Breath Condensate in Humans. *American Journal of Respiratory and Critical Care Medicine* [online]. 2001, **164**(5), 731-737 [cit. 2020-04-23]. DOI: 10.1164/ajrccm.164.5.2101032. ISSN 1073-449X.

CRUICKSHANK-QUINN, Charmion, Michael ARMSTRONG, Roger POWELL, Joe GOMEZ, Marc ELIE a Nichole REISDORPH. Determining the presence of asthma-related molecules and salivary contamination in exhaled breath condensate. *Respiratory Research* [online]. 2017, **18**(1) [cit. 2020-04-23]. DOI: 10.1186/s12931-017-0538-5. ISSN 1465-993X.

KONSTANTINIDI, Efstathia M., Andreas S. LAPPAS, Anna S. TZORTZI a Panagiotis K. BEHRAKIS. Exhaled Breath Condensate: Technical and Diagnostic Aspects. *The Scientific World Journal* [online]. 2015, **2015**, 1-25 [cit. 2020-04-23]. DOI: 10.1155/2015/435160. ISSN 2356-6140.

BANNIER, Michiel A. G. E., Philippe P. R. ROSIAS, Quirijn JÖBSIS a Edward DOMPELING. Exhaled Breath Condensate in Childhood Asthma: A Review and Current Perspective. *Frontiers in Pediatrics* [online]. 2019, **7** [cit. 2020-04-23]. DOI: 10.3389/fped.2019.00150.

WALLACE, M. Ariel Geer a Joachim D. PLEIL. Evolution of clinical and environmental health applications of exhaled breath research: Review of methods and instrumentation for gas-phase, condensate, and aerosols. *Analytica Chimica Acta* [online]. 2018, **1024**, 18-38 [cit. 2020-04-23]. DOI: 10.1016/j.aca.2018.01.069. ISSN 00032670.

Vedoucí bakalářské práce: **prof. Juan Bautista De Sanctis, PhD.**
Ústav molekulární a translační medicíny

Datum zadání bakalářské práce: **24. dubna 2020**
Termín odevzdání bakalářské práce: **31. července 2021**

UNIVERZITA PALACKÉHO V OLOMOUCI
PŘÍRODOVĚDECKÁ FAKULTA
KATEDRA BUNĚČNÉ BIOLOGIE A GENETIKY
Šlechtitelů 27, 783 71 Olomouc – Holice
tel.: +420 585 634 901
-2- - 7 -04- 2021

L.S.

doc. RNDr. Martin Kubala, Ph.D.
děkan

prof. RNDr. Zdeněk Dvořák, DrSc.
vedoucí katedry

V Olomouci dne 7. dubna 2021

Bibliographical identification

Author's first name and surname: Kamila Baslarová

Title: Lipidomic analysis of exhaled breath condensate

Type of thesis: bachelor

Department: Department of Cell Biology and Genetics, Faculty of Science Palacký University Olomouc

Supervisor: prof. Juan Bautista de Sanctis, Ph.D.

The year of presentation: 2021

Keywords: lipidomics, exhaled breath condensate, ceramides, ergosterol, mass spectrometry

Number of pages: 56

Number of appendices: 0

Language: English

SUMMARY

Exhaled breath condensate collection is a method for obtaining the biomarkes from respiratory tract. Ceramides are signalling molecules and structural elements of the cell membrane. They are involved in inflammatory proceses. Ergosterol is a sterol present in cell membranes of Fungi. It can be a marker of Fungi infection. In this thesis we collected exhaled breath condensate of 23 healthy volunteers in order to quantify and corelate the levels of ceramides and ergosterol. We detected significant positive correlation between ergosterol and very long chain ceramides C24:1 and significant negative correlation between ergosterol and very long chain ceramide C26. We also reported that ceramide content may depent on the gender, since ceramide C18:1 was elevated in females and ceramide C24:1 was elevated in males.

Bibliografické údaje

Jméno a příjmení autora: Kamila Baslarová

Název práce: Analýza lipidů v dechovém kondenzátu

Typ práce: bakalářská

Pracoviště: Katedra buněčné biologie a genetiky, PřF UP v Olomouci

Vedoucí práce: prof. Juan Bautista de Sanctis, Ph.D.

Rok obhajoby práce: 2021

Klíčová slova: lipidomika, dechový kondenzát, ceramidy, ergosterol, hmotnostní spektrometrie

Počet stran: 56

Počet příloh: 0

Jazyk: Anglický

ABSTRAKT

Odběr dechového kondenzátu je metoda sběru biomarkerů z dýchacích cest. Ceramidy jsou signální molekuly a také strukturní komponenty buněčných membrán. Hrají roli v zánětlivých procesech. Ergosterol je sterol vyskytující se v buněčných membránách hub. Může být markerem infekce způsobené patogenem z říše hub. V rámci práce jsme odebrali vzorky dechového kondenzátu dvaceti třem zdravým dobrovolníkům za účelem kvantifikace a korelace ceramidů a ergosterolu. Detekovali jsme signifikantní pozitivní korelaci mezi ergosterolem a ceramidem C24:1 a signifikantní negativní korelaci mezi ergosterolem a ceramidem C26. Rovněž jsme pozorovali zvýšenou hladinu ceramidu C18:1 u žen a zvýšenou hladinu ceramidu C24:1 u mužů.

DECLARATION

I declare that this bachelor thesis was written independently with the help of my supervisor, prof. Juan Bautista De Sanctis, PhD., and using the sources listed in the reference.

In Olomouc…… ……..

Kamila Baslarová

ACKNOWLEDGMENT

I would like to thank my supervisor prof. Juan Bautista de Sanctis, PhD. for professional work management and valuable advice that helped me complete this work.

CONTENT

ABBREVIATIONS

Acid sphingomyelinase	ASM
Autocrine motility factor	AMF
Ceramide kinase	CERK
Ceramide-1-phosphate	C1P
Ceramidases	Asah1
Ceramide synthase	CerS
Ceramide transfer protein	CERT
Chronic obstructive pulmonary disease	COPD
Coenzyme A	CoA
Cystic fibrosis	CF
Cystic fibrosis transmembrane conductance regulator	CFTR
C1P transport protein	CPTP
Desaturase	Degs
Ductal carcinoma in situ	DCIS
Electrospray ionization	ESI
Endoplasmatic reticulum	ER
Exhaled breath condensate	EBC
Four-phosphate adaptor protein	Fapp2
Fractionated exhaled nitric oxide	FeNO
Glucosylceramide synthase	Ugcg
Golgi apparatus	GA
Glycosylphosphatidylinositol	GPI
GPI-anchored green fluorescent protein	GPI-GFP
Inhibitor 2 of protein phosphatase 2A	I2PP2A
Insulin-like growth factor-1	IGF-1
Interleukin-6	IL-6
3-ketosphinganine reductase	Kdsr
Lactosyl Ceramide	LacCer
Matrix-assisted laser desorption ionization	MALDI

MAPK/ERK kinase kinase 1	MEKK1
Mass spectrometry	MS
Phosphatase 2A	PP2A
Protein kinase C ζ	PKCζ
Serine palmitoyltransferase	Sptlc
Sphingomyelin synthase	Sgms
Sphingosine1-phosphate	S1P
Sphingosine kinase	Sphk1
Stress-activated protein kinase	SAPK
Tumor necrosis factor α	TNF-α

FIGURES

TABLES

GRAPHS

1 INTRODUCTION

The thesis focuses on the lipidomic analysis of the exhaled breath condensate. The molecules of interests are ceramides, which have never been analyzed in this kind of sample. Because ceramides are structural and signalling molecules that participate in inflammatory processes, their equilibrium in exhaled breath condensate may reflect the conditions of patient´s airways. Another analyzed compound is ergosterol, a sterol present in cell membranes of the fungi. Fungi spores are omnipresent and can impact our respiratory tract causing a fungal infection. Hence, the thesis aims to quantify the levels of ceramides and ergosterol in exhaled breath condensate. The role of ceramides and ergosterol as potential biological markers will be discussed.

2 AIMS OF THE THESIS

Quantification of ceramides in exhaled breath condensate.

Quantification of ergosterol in exhaled breath condensate.

Correlation of the ergosterol and ceramide content in exhaled breath condensate.

Discusse the role of role of ceramides and ergosterol as potential biological markers.

3 LITERATURE REVIEW

3. 1.1 SPHINGOLIPIDS

Sphingolipids are a lipid class that was first discovered in brain tissue. They are the critical part of phospholipid membranes and signal molecules – intracellular second messengers and extracellular mediators. Their signalling depends on all kinds of stimuli, from inflammation to stress. They can be quickly synthesized. The sphingolipid pathway has a de novo synthesis and two anabolic pathways that allow the formations of new structures from existing ones. (Yang et Uhlig, 2011).

The backbone of sphingolipids consists of the hydrophobic part known as a sphingoid base and the hydrophilic part. A sphingoid base is usually 16 carbons long, and it forms an amide bond that connects the base to the fatty acid. The base can be represented by sphingosine (2-amino-4-trans-octadecene-1,3-diol) or sphinganine ((2S,3R)2-aminooctadecane-1,3-diol) etc. Hydrophilic parts may vary. In the simplest sphingolipids (e.g. ceramides) they are represented only by hydroxyl groups. Phosphates and sugar residues are part of more complex sphingolipids structures (e.g. sphingomyelin, cerebroside) (Yang et Uhlig, 2011).

The synthesis of sphingolipids occurs in the membrane of the smooth endoplasmic reticulum (ER) and in the Golgi apparatus (GA). Enzymes called serine palmitoyltransferases (Sptlc1and Sptlc2) process palmitic acid and serine to form 3-ketosphinganine. Another ER membrane enzyme known as 3-ketosphinganine reductase (Kdsr) reduces 3-ketosphinganine to sphinganine. The next step of this pathway is acylation of sphinganine which is catalyzed by one of the six ceramide synthases (CerS1–6) that have been characterized in vertebrates (Yavin et Gatt, 1969) (Sribney, 1966). Each of the six CerS utilizes fatty acids with different carbon number coupled with coenzyme A (CoA). The range is wide. The shortest fatty acid used by CerS can be 14 carbons long, and the longest one can be 26 carbon long. The CerS1 processes acyl-CoA with 18C fatty acid residue. The CerS2 processes acyl-CoA with 20C, 22C, 24C and 26C fatty acid residues. The CerS3 processes acyl CoA with 22C, 24C and 26C fatty acid residues. The CerS4 processes acyl CoA with 18C and 20C fatty acid residues. The CerS5 processes acyl-CoA with 16C fatty acid residue. The Cers6 processes acyl CoA with 14C and 16C fatty acid residues (Mizutani et al, 2005). The products of this part of the synthesis are dihydroceramide with various lengths of the acyl side chains. Based on this parameter, ceramides can be classified as long-chain ceramides (C14:0–C20:0), very-long-chain ceramides (C22:0–C26:0) and ultra-long-chain ceramides (> 26 carbons). The synthesis of ceramides

is completed by one of the desaturases which are located in the ER (Degs1 and Degs2) (Gárić et al., 2019).

The ceramide transport from the smooth ER into the GA is maintained by the ceramide transfer protein (CERT). Only C14, C16, C18, and C20 ceramides and their derivates can be effectively transported by CERT (Kumagai et al, 2005). The mechanism transporting very-long-chain ceramides from ER to plasma membrane is unknown (Garić et al, 2019). Ceramides can also be transported inside the vesicles. However, ceramides from vesicular transport are not used in the sphingolipid synthesis. They are a substrate for glucosylceramide synthesis. CERT transport's ceramides are utilized by sphingomyelin synthases (Sgms1 and Sgms2), which form sphingomyelin by binding phosphatidylcholine onto the primary hydroxyl group of ceramides (Hanada et al., 2003). More complex glycosphingolipids are as well synthesized in the GA by the glucosylceramide synthase (Ugcg). Ugcg produces precursor glucosylceramides. They are then transported by four-phosphate adaptor protein (Fapp2) into the trans-Golgi, where the glycosphingolipids synthesis is completed (Garić et al, 2019).

The sphingomyelins can be converted to ceramides by a family of enzymes called sphingomyelinases. We distinguish acid, neutral, and alkaline sphingomyelinase. Each of them has a different pH optimum for activity. The acid sphingomyelinase (ASM) plays a part in the cell response to the infection (Henry et al., 2013).

Ceramides are also processed in the synthesis of ceramide-1-phosphate (C1P). The phosphate binds to the OH group originated from serine. This reaction is catalyzed by ceramide kinase (CERK) (Lamour et al., 2007). C1P is then transported to the cell membrane by C1P transport protein (CPTP) (Simanshu et al., 2017).

Ceramidases (Asah1, Asah2, Acer1, Acer2) are enzymes that degrade ceramides to obtain sphingosine. Sphingosine can be turned to sphingosine1-phosphate (S1P) by phosphorylation which is maintained by sphingosine kinases (Sphk1 and Sphk2) (Stoffel et al., 1968). Sphk1is located in the plasma membrane. Sphk2 is located in the nucleus. (Garić et al., 2019). S1P serves as a signalling molecule to decrease the inflammatory response, and it is essential in proper embryonic angiogenesis. And it has a wide spectrum of impact on the blood cells (Kono et al., 2004). For details of sphingolipid synthetis see Figure 1.

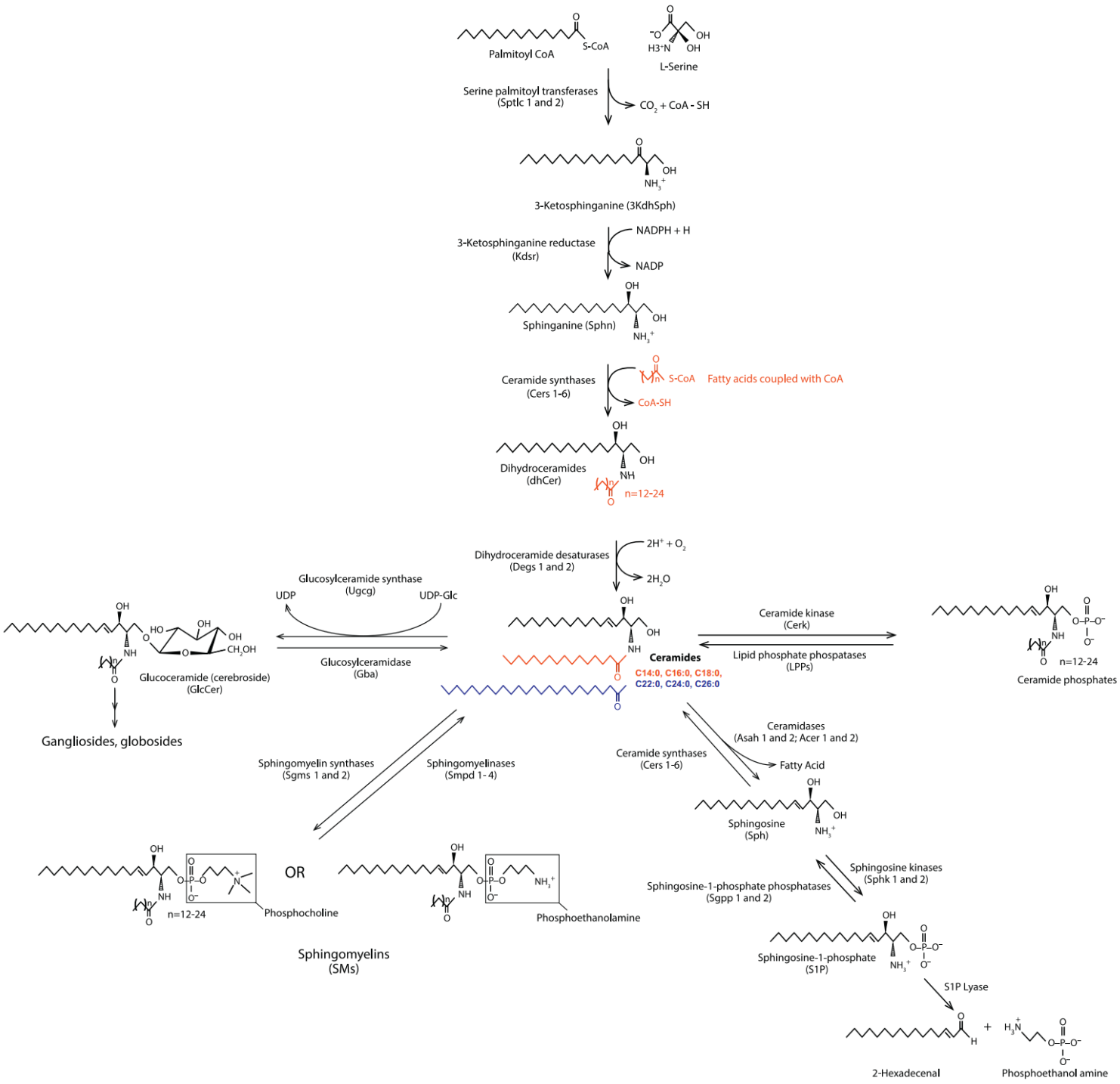

Figure 1 – Biosynthesis of ceramides and other sphingolipids

According to Gárić et al., 2019

3.1.2 CERAMIDES

Firstly, ceramides are a vital part of phospholipid membranes. They form lipid rafts which are more stable than the rest of the membrane partially because of cholesterol. Also, sphingolipid's acyl chains are usually more saturated than the acyl chains of the rest of the lipids in the membrane. At low temperature, 4 °C, the lipid rafts are resistant to various detergents like Triton-X or Brij-98 (Schuck et al., 2003). Many proteins are associated with lipid rafts e.g. proteins with a glycosylphosphatidylinositol (GPI) anchor, and their extraction impacts the lipid raft structure (Brown et Rose, 1992) (Skibbens et al., 1989). The lack of cholesterol or sphingolipids facilitates the dissolution of proteins associated with lipid rafts (Hanada et al., 1995). There are two types of lipid rafts; the planar or non-caveolar and the calveolar. The caveolae lipid rafts form tube-like invaginations in the membrane known as calveolins (Lingwood et Simons, 2009) (Rothberg et al., 1992). The caveolae lipids rafts are a part of a process known as clathrin-independent endocytosis, particularly endocytosis via caveolae. This process internalizes, e.g. certain virus particles, cholera and tetanus toxin, folic acid, serum albumin, autocrine motility factor (AMF), alkaline phosphatase, GPI-anchored green fluorescent protein (GPI-GFP), and the bodipy-labelled glycosphingolipid Lactosyl Ceramide (LacCer) (Pelkmans et Helenius, 2002) (Montesano et al., 1982) (Rothberg et al., 1990) (Schnitzer et al., 1994) (Benlimame et al., 1998) (Parton et al., 1994) (Nichols et al., 2001) (Puri et al,. 2001). The equilibrium of ceramides in the phospholipid membrane determines membrane permeability. Membranes with increased content of long-chain ceramides are more permeable for water than membranes with increased content of very-long-chain ceramides (Pullmannová et al. 2017).

Ceramides play a part in the process of apoptosis. In radiation-induced apoptosis, elevated levels of ceramide C16:0 were found in sensitive Jurkat cells and not in radioresistant K562 cells. Moreover, the concentration of ceramide C16:0 in Junkart cells increased with radiation exposure time (Thomas et al, 1999). Elevated ceramide C16:0 levels had been reported in the tumor necrosis factor α (TNF-α) treated Ad5IκB-infected apoptotic hepatocytes from rats and mouses cell lines (Osawa et al, 2005). Therefore, ceramides may play an vital role in apoptosis induction.

Cell proliferation also involves ceramide synthesis. However, the effects of long-chain ceramides and very-long-chain ceramides may vary. A study performed on MCF-7 and HCT-116 cell lines in which various type of CerS were overexpressed, CerS4 and CerS6, which leads to an increased level of long-chain ceramides, contributed to mitochondrial damage and

apoptosis or necrosis and thus inhibition of the cell proliferation (Hartmann et al, 2012). A long chain ceramide C16:0 induces changes in the mitochondria membrane that release cytochrome c and induce apoptosis (Siskind et al., 2002). On the other hand, mitochondria of overnight-starved male rats exposed to the mixed C22:0 and C16:0 ceramides showed less damage than the treatment with a single ceramide (Stiban et Perera, 2015). Therefore, the equilibrium of ceramides may have a significant impact on cell proliferation.

Phosphatase 2A (PP2A) enzymes are Ser/Thr phosphatases that mean they remove phosphate from serine and threonine residues of target proteins and regulate several cellular functions. Ceramides regulate (PP2A) activity by binding to the inhibitor 2 of protein phosphatase 2A (I2PP2A). Studies also suggested that I2PP2A has more affinity towards ceramide C18:0 than ceramide C16:0 (Mukhopadhyay et al., 2008) (Saddoughi et al., 2013). For example, PPA2 enzymes dephosphorylate c-Myc transcription factor (Yeh et al., 2004), which is then ubiquitinated. Constitutive overexpression of c-Myc is present in various types of tumors (Spencer et Groudine, 1991).

Another enzyme affected by the activity of ceramides is protein kinase C ζ (PKCζ). This atypical protein kinase is involved in cancer development, cell proliferation and junction formation (Islam et al., 2018) (Suzuki et al., 2001). It has been suggested that higher expression and activation of PKCζ is involved in developing invasive and metastatic breast cancers. The PKCζ depleted cells struggled to form metastasis (Paul et al., 2015). Loss of PKCζ generates an overproduction of interleukin-6 (IL-6) and, in turn, tumorigenesis, as observed in Ras-induced lung adenocarcinoma in mice (Galvez et al., 2009). Ceramide C16:0 binds PKCζ and contributes to activate the signalling cascade with MAPK/ERK kinase kinase 1 (MEKK1), SEK, and stress-activated protein kinase (SAPK). This cascade inhibits insulin-like growth factor-1 (IGF-1), leading to cell cycle arrest (Bourbon et al., 2000).

The importance of CerS and their ceramide products were studied in CerS knockout mice. The CerS1mutants suffered from progressive ataxia, loss of cerebellar Purkinje cells and abnormal cumulation of lipofuscin within neurons. The mice were smaller and hyperactive. However, the lifespan of CerS1 deficient mice wasn't significantly shortened in comparison with the lifespan of wild type mice (Zhao et al., 2011).

The CerS3 is vital for the proper development of the skin. The KO mice lacked sphingolipids with ultra-long-chain fatty acid residues. They had discontinuous extracellular lipid lamellae and changes within a cornified cell envelope structure that replaces the plasma membrane in differentiated keratinocytes. Those changes included unmasked loricrin, which is a protein forming a vast majority of the cornified cell envelope, hyperkeratosis, persistence

of periderm and non-peripheral corneodesmosomes, which are structures derived from desmosomes. Their degradation is necessary for desquamation. The mice also displayed a defect in the processing of profilaggrin, which is the precursor of filaggrin – skin protein contributing to the formation of skin barrier by interaction with intermediate filaments (Ishitsuka et Roop, 2020) (Bernadrd et al., 2001) (Steiner et al., 1981) (Sakabe et al., 2013). The lack of CerS3 and its products in those mice led to lethal transepidermal water loss (Jennemann et al., 2012). Another study shows that Cers3 is essential for spermatogenesis. Lack of CerS3 product during spermatogenesis leads to enhanced apoptosis during meiosis and the formation of multinuclear giant cells. It can also lead to spermatogenic arrest (Rabionet et al., 2015).

The CerS4 knockout mice displayed alopecia due to the hair canal blocking caused by sebum with impaired function due to the changes in lipid composition. The CerS2 is partially capable of replacing the CerS4 in ceramide production. However, the levels of sphingomyelins synthetized from ceramide C18:0 and C20:0 were lowered in the dermis and the levels of sphingomyelins derived from C16:0 were higher than in the wild type mice (Ebel et al., 2014).

The CerS5 knockout mice do not show any significant phenotype differences in comparison with the wild mice. However, the CerS5 maintains the usual levels of ceramide C16:0 within the lungs, spleen, muscle, liver, and white adipose tissue. Interestingly, the CerS5 knockout mice mutants on a high-fat diet did not become insulin-resistant like wild-type mice. The insulin levels in blood serum of CerS5 knockout mice on high-fat diet and CerS5 knockout mice on low-fat diet were lower than those in wild-type mice. High-fat diet also leads to autophagy within tissues in wild type mice and not in Cers5 knockout mice. Thus, CerS5 possibly plays a part in obesity, insulin resistance and adipose tissue inflammation (Gosejacob et al, 2016).

The effects of the lack of CerS6 activity are similar to those of lack of CerS5 activity. In CerS6 KO mice, mitochondria incorporation of palmitoyl-CoA is deficient, along with the concentration of ceramide C16:0 in different organs (Ebel et al., 2013). CerS6 KO mice showed increased resistance to high-fat diet as the CerS5 deficient mice. The CerS6 knockout mice had reduced adipocyte size, lower serum leptin concentrations, lower macrophage adipose tissue infiltration, and inflammatory cytokine production. The expression of CerS6 in white adipose tissue positively correlates with body mass index, hyperglycemia and body fat content in humans and negatively correlates with glucose infusion rate during euglycemic-hyperinsulinemic clamps that means higher CerS6 expression correlates with insulin resistance.

The ceramides C14:0–C18:0, C22:0 and sphingomyelins were also increased in obese participants of the study (Turpin et al., 2014). However, the mice lacking CerS6 activity developed a condition known as clasping abnormality in the hind limbs that can indicate impaired motoneuronal functions (Cuellar et al., 2008). This hypothesis was also supported by the horizontal wire test (Ebel et al, 2013).

The deficiency of CerS2 has more profound effects on the mammal organism. It was also studied on mice. The levels of very long-chain ceramides were reduced, and the levels of long-chain ceramides like ceramide C16:0 were increased in liver, kidneys and lungs in mice and in transformed human lung cells (Petrache et al., 2013). Furthermore, the liver of the mice developed hepatomegaly at the age of 4 months and then hepatocarcinoma at the age of 7 months (Pewzner-Jung et al., 2010). The kidneys were also impacted by the formation of discrete gaps in renal parenchyma.

The deficiency of CerS2 also causes myelin destabilization. Around 9 months of age it leads to degeneration of the medullary tree and the internal granular layer of the cerebellum, which is manifested by the formation of microcysts (Imgrund et al., 2009). The CerS2 is the most abundant type of CerS in the lungs. Therefore, the lungs of CerS2 knockout mice displayed patchy areas of perivascular inflammation and accumulation of alveolar macrophages in the airspaces. Also, the levels of macrophages in the bronchoalveolar lavage fluids of those mice have elevated, and the levels of lymphocytes and neutrophils in the airways (Petrache et al., 2013). These conditions caused by long-chain and very-long-chain ceramides imbalance within impacted mice do not protect the animals from respiratory infections.

On the other hand, the inflammatory environment contributes to the onset of bacterial respiratory infection. This effect has been observed on CerS2 knockout mice and on patients with cystic fibrosis (CF), which is an autosomal recessive disease with an impact on cystic fibrosis transmembrane conductance regulator (CFTR) (Riordan et al., 1998). CFTR is a membrane protein, specifically a chlorine channel (Liu et al., 2017). If it malfunctions, the transepithelial movement of water is slowed down. The lack of CFTR leads to thickening of the surfactant in the lungs and mucus in the intestines and other secretions in sinuses, pancreas, hepatobiliary tree, and vas deferens. Patients with CP prone to suffer from respiratory infection, which can endanger their lives. Samples from airway epithelial, tracheal, and bronchial cell from CerS2 null mice, CF mice and nasal epithelial cell samples from CF patients had lower levels of sphingosine. The CerS2 null mice had also increased levels of ceramides. If the CerS2 null mice and the CF mice were supplemented with sphingosine via inhalation,

they did not develop a severe infection after being treated with *Pseudomonas aeruginosa* (Pewzner-Jung et al., 2014).

CerS are capable of forming dimers and regulating their activity due to this action. Studies presented an explanation that the substrate binding to one CerS monomer allosterically affects substrate binding to the other one. Either homodimers or heterodimers can be formed. The activity of CerS5 is inhibited after coexpression in a homodimer with catalytically inactive CerS5. The activity of CerS2 is enhanced by coexpression with catalytically inactive CerS5 or CerS6. CerS5 and CerS2 heterodimers produce very-long-chain ceramides. CerS5 homodimers produce long-chain ceramides (Laviad et al., 2012).

3.1.3 SHINGOLIPIDS AND CERAMIDES WITHIN LUNGS DISEASE

Sphingolipids play an essential role in lung development, and they are critical to surfactant production. Mammal lungs maintain a specific lipid-protein layer which changes its composition during fetal development. Among other compounds of this layer, we may find lecithin and sphingomyelin. Their ratio is crucial in the diagnosis of fetal lung maturity. It can be analyzed using amniotic fluid since the lipids in the fluid reflect the lipids in the fetus's lungs. If the ratio is below 2 the infant will have the risk of neonatal respiratory distress syndrome. The neonatal respiratory distress syndrome results from insufficient production of surfactant that leads to higher alveolar surface tension causing breathing difficulties which can lead to pneumothorax or lung collapse (Gluck et al., 1971) (McPherson et Wambach, 2018).

Ceramide levels are elevated when the lungs are exposed to reactive oxygen and nitrogen species. The oxidative stress caused by hydrogen peroxide upregulates neutral sphingomyelinase 2, more sphingomyelin is produced and consequently more ceramide. This event leads to hydrogen-induced apoptosis. Cigarettes smoke has similar effects on ceramide levels and lung cell apoptosis (Goldkorn et al., 1998) (Levy et al., 2009).

When the lung cells are exposed to NO, reactive nitrogen species, the ceramide levels increase, but apoptotic cells do not. NO induces the activity of CerS, so ceramides are synthesized *de novo.* However, NO also stimulates interaction between acid sphingomyelinase and caspase-3. Caspase-3 is a protease involved in DNA fragmentation, nuclear condensation, and membrane blebbing (Enari et al., 1998) (Sahara et al., 1999) (Sebbagh et al., 2001). Therefore, oxidative stress caused by reactive oxygen and nitrogen species induces apoptosis in lung cells via ceramides generated by various metabolic pathways. This process may be a mechanism by which ceramide metabolism impacts the lung diseases associated with cigarette smoking and air pollution.

Ceramide rich lipids rafts tend to spontaneously form larger platforms (Nurminen et al., 2002). These platforms change the membrane properties since they contribute to the entrapment and clustering of receptors and intracellular signalling molecules. This effect is made possible by the interaction between the entrapped receptors and ceramides enriched domains. The entrapment would be energetically unfavourable in membrane regions without such concentrations of ceramides (Grassmé et al., 2001, 2003A, B) (Bock and Gulbins, 2002). The high density of receptors in this part of the membrane is very effective in signalling. Interestingly, these platforms are formed to respond to various stimuli including infections with pathogens such as *Pseudomonas aeruginosa, Neisseriae gonorrhoeae, Neisseria meningitides,*

rhinovirus, and measles virus (Grassmé et al., 2003A) (Grassmé et al., 1997) (Simonis et al., 2014) (Grassmé et al., 2005) (Gassert et al., 2009) (Avota et al., 2011) (Seitz et al., 2015). After the infection by e.g. *Pseudomonas aeruginosa* the acid, sphingomyelinase is activated and translocated onto outer layer of the plasma membrane (Grassmé et al., 2003A) (Zhang et al., 2008). Acid sphingomyelinase produces ceramides from sphingomyelins and attracts receptors and enzymes which are important for the defense against pathogen e.g. NADPH-oxidases which produce reactive oxygen species, and CD95 receptor, which is involved in *Pseudomonas aeruginosa* mediated cell death (Grassmé et al., 2000) (Grassmé et al., 2003A) (Zhang et al., 2008) (Zhang et al., 2010). The sphingomyelinase-deficient mice or cells with sphingomyelinase inhibition are more susceptible to pulmonary infections caused by *Pseudomonas aeruginosa* (Grassemé et al, 2003A). The destruction of the lipid rafts alone also worsens *Pseudomonas aeruginosa* by host cells (Kowalski and Pier, 2003). Other studies on *Listeria monocytogenes* showed the importance of the sphingomyelinase/ceramide system (Cossart et al., 1989). The sphingomyelinase deficiency makes the organism more susceptible to *Listeria monocytogenes* infection. It is believed that it impairs the mechanism of the fusion of *Listeria monocytogenes*-containing late phagosomes with lysosomes (Utermöhlen et al., 2003). However, mice who lack acid sphingomyelinase are more resistant to Mycobacterium avium infections (Utermöhlen et al., 2008), and the mechanism is not fully understood. In conclusion, the sphingomyelinase/ceramide system is essential in the physiological and pathological response to pathogens.

Chronic lung diseases also modify the lipidomic profile of the patients. In asthma, ceramides are related to airflow obstruction, bronchial hyperresponsiveness, and underlying inflammation. Asthma is further classified based on clinical characteristics, biomarkers, lung physiology, genetics, histopathology, epidemiology, and treatment response according to specific guidelines (ARIA).

The most common endotype of asthma is allergic asthma. Its symptoms include specific allergic bronchospasms after exposure to the allergen. Allergens also trigger the subsequent inflammatory cell influx, typical of the late asthmatic response. A common feature of asthma patients is allergic rhinitis which is also associated with IgE levels. However, airway inflammation is usually detected by spirometry before and after a bronchodilator, and by fractionated exhaled nitric oxide (FeNO). FeNO levels are clinically valuable indicators of the inflammatory burden in the airways (Lötvall et al., 2011).

Sphingolipid levels were analyzed in plasma of the house dust mite allergic asthmatic and rhinitis patients. Allergic reaction and allergen-induced asthma of the patients were

triggered intrabronchially with *Dermatophagoides pteronyssinus* extract. During the early asthma response, the levels of S1P were increased in the house dust mite allergic asthmatic patients, who developed late asthmatic response in the future. Thus, the lipidomic profile in this asthma endotype impacts the severity and length of the reaction to the allergen. (Kowal et al.,2019).

Another lung disease in which the metabolic profile has been studied is chronic obstructive pulmonary disease (COPD). It is defined by irreversible air inflow limitation, which worsens over time because of damage to the airway and lung parenchyma due to chronic inflammation (Yoon et al., 2017). COPD develops in the susceptible lungs after their long-time exposure to environmental stimuli like household air pollution or tobacco smoking. However, COPD can also be induced by infection. This disease is progressive, but treatment and preventions are possible. Studies also suggested that e-cigarette smoking may alter the metabolome of human bronchial epithelial cells. Toxins that are present in cigarette smoke are also detectable in e-cigarette vapour. Therefore, e-cigarette smoking may contribute to COPD development, and it can´t be considered harmless if this link will be confirmed (Aug et al., 2015).

Various COPD phenotypes are distinguishable base on the rate of airflow obstruction, emphysema, chronic bronchitis, and frequent exacerbations. Emphysema is the destructive and permanent enlargement of distal airspaces and alveolar walls, ultimately leading to impaired oxygenation (Snider et al., 1985). In an emphysema model in laboratory animals induced by blocking VEGF receptor, the levels of ceramides are increased (Kasahara et al., 2000). If ceramide de novo synthesis is inhibited, the apoptosis induced by blocking the VEGF receptor decreased. In the same study, the authors also analyzed levels of ceramides in smokers with emphysema. In comparison with healthy controls, the ceramides of smokers with emphysema were increased, particularly in alveolar septal cells and alveolar macrophages. Ceramides levels of smokers without emphysema were also altered. Therefore, maintaining an optimal balance of lung ceramides is important because its alternations are linked to the development of pro-inflammatory and apoptotic conditions that can lead to emphysema like symptoms (Petrache et al., 2005).

Another study focused on which changes within the lipidomic profile in the patient´s plasma are detectable in various COPD phenotypes (Bowler et al., 2015). Plasma ceramides in patients with emphysema were lowered. The authors propose that decreased plasma ceramide levels may be caused by increased sphingomyelinase activity and other components of ceramide recycling pathways. Other sphingolipids that negatively correlated

with the emphysema phenotype were gangliosides and sphingomyelins. Trihexosylceramide is positively associated with frequent COPD exacerbations. A significant correlation of specific sphingolipids with the rest of the COPD phenotypes wasn´t detected in the study (Bowler et al., 2015).

According to presented studies, ceramides are closely linked to lung disease, and they can serve as a marker of pathogen invasion or oxidative stress induce by pollutants. To test this hypothesis, we analyzed the levels of ceramides in exhaled breath condensate (EBC) by mass spectrometry. The thesis aims to test if EBC analysis can serve as a noninvasive method for detecting airway inflammation and perhaps reduce the necessity of invasive procedures such as bronchoalveolar lavage and lung biopsy.

3.2 MASS SPECTROMETRY

Mass spectrometry (MS) is a qualitative and quantitative laboratory method that analyzes ions based on their mass to charge ratio (m/z). It was invented in the late 1880s, and at first, it was only used to analyze volatile compounds with a molecular weight under 1000 Da. Nowadays, the method is usually combined with HPLC or gas chromatography.

In order to undergo analysis, the substance needs to be ionized. This can be done by soft ionizing methods or hard ionizing methods. Soft methods transfer the minimum internal energy on the analyte in the process compared to the hard methods. The oldest ionizing method used was the electron beam which impacts the analyte in the vacuum. The analyte needs to be in the gas phase to be ionized by this process. The electrons are generated by thin heated metal wire. They interact with the volatile particles in the gas, turning them into radical cations. This process can be replaced by chemical ionization or plasma desorption which are classified as soft ionizing methods. They produce molecular ions and not radical cations, which is convenient because molecular ions are more stable. The principle of chemical ionization is the ionization of neutral molecules like methane by electrons. Later the ionized molecules interact with the sample turning it into ions. Both electron beam ionization and chemical ionization can be used only with samples with a molecular weight under 1000 Da. The plasma desorption ionizes samples up to 100 000 Da of molecular weight.

Another soft ionizing technique is electrospray ionization (ESI). To perform ESI the analyte needs to dissolve in a polar buffer and spray it into the chamber using a thin needle with electrical potential; the solvent with analyte are nebulized. The mist is then exposed to warm neutral gas in order to vaporize and release ions. Two theories of ESI describe this step. The first theory is ion evaporation method. The ions are dispersed into the gas phase thanks to Columbic forces, which eventually exceed the shrinking droplets' surface tension. This theory would accurately describe the process for ions with m/z ratio lower than 30. Another theory, called the charge residue model, explains the ion release for ions with m/z ratio over 30. The droplets vaporization is combined with the droplets fragmentation, resulting in multiple charged ions releasing into the gas phase. ESI can be used on ions with a wide range of molecular weight. Since ESI operates with solutions, it is commonly used to process the samples separated in liquid chromatography.

The technique called matrix-assisted laser desorption ionization (MALDI) is broadly used in the analysis of DNA (Gut, 2004), lipids (Balazy, 2004) and glycoconjugates (Harvey, 1999). This technique is similar to the laser beam impact. However, the analyte is dissolved in a solvent and then mixed with a matrix which is then dried. The matrix is then impacted by a laser beam which releases the ions of the analyte. The matrix block can be placed in a vacuum. However, MALDI in atmospheric pressure is also possible (Laiko et al., 2000).

After the sample is ionized, the ions need to be separated based on their m/z ratio. This is a task performed by mass analyzers. There are three basic analyzer types: quadrupole analyzer, time of flight analyzer and quadrupole ion trap analyzer.

The quadrupole analyzer was invented by Wolfgang Paul – laureate of the Nobel prize. (Paul et Steinwedel, 1956). It consists of four-rod electrodes that are parallel to each other. The two opposite electrodes have a positive DC voltage (U); the other two have a negative DC voltage (U), and all the rods have AC potential with high radiofrequency. Ions oscillate at the centre of the quadrupole axis. The quadrupole is set to release only ions with a certain m/z ratio. Ions with different m/z ratios are deflected from their trajectory, and they end up on the quadrupole rods. The amplitude and voltage of the electrodes change over time, although their ratio remains stable. Gradually all ions m/z ratio categories are released from the quadrupole filter onto the detector. However, the quadrupole analyzer is only suitable for analysing ions with a molecular weight under 4000 Da. This problem can be prevented by using more quadrupoles lined up in a row or by the use of the quadrupole in combination with the time of flight analyzer.

The principle of the time of flight analyzer is that the ions with different m/z ratios will fly the same trajectory at various times after being accelerated with the same energy of a voltage pulse. It consists of 1–2 m long tube which does not contain any magnetic or electric field. The problem with this type of analysis is that the ions do not enter the tube all at once. The solution is to equip the tube with an electrostatic ion mirror, an electric field in the ion´s trajectory. Ion is supposed to bounce back from the electrostatic ion mirror, change its direction, and continue to the detector. Ions with higher kinetic energy go deeper into the mirror's electric field, and they are slowed down compared to the ions with lower kinetic energy. Therefore, the differences between ions are balanced, and the time of their flight to the detector depends primarily on their m/z ratio. Another detector can be placed behind the mirror to detect the ions that get through. Time of flight analyzer can analyze a wider range of molecules based on their molecular weight, up to kDa.

The ion trap analyzer was also introduced by Wolfgang Paul and his team (Paul et Steinwedel, 1956). And because of it the two most common types of ion traps are referred as Paul trap. We distinguish quadrupole/cylindrical (or 3D) and linear (or 2D) Paul trap. The 3D trap has one central ring electrode and two isolated side electrodes. The ions get inside the trap through the opening in the middle of one of the side electrodes. They are delivered there thanks to a voltage pulse and then they are trapped inside because of the voltage on the central ring electrode. Then they proceed through the opening in the second side electrode onto the detector. They are released based on their m/z ratio due to the electrode´s voltage change. The 2D trap has two isolated side electrodes and four parallel cylindrical electrodes. It is more effective than the 3D trap (Arevalo et al., 2020).

Apart from the single-stage mass spectrometry with one analyzer, the tandem mass spectrometry utilises a whole set of analyzers. For example, the triple quadrupole instrument consists of one quadrupole which selects the targeted ions, a collision cell where the ions collide and fragment, and second quadrupole which selects the fragmented ions. Also, the combination of three to two quadrupoles and one time of flight analyzer is commonly used. This type of mase spectrometry can be combined with ESI or MALDI with a little manipulation of the configuration, and it has higher sensitivity compared to triple quadrupole (El-Anned et al., 2009).

The MS detectors can be an electron multiplayer, a photomultiplier – the ions hit the phosphor plate, which emits photons, or a Faraday cage.

The collected data from the mass spectrometer are presented in the form of MS spectrums where the x-axis represents the m/z ratio and the y-axis the relative intensity. The highest peak

represents 100 % intensity. The spectra are unique for the analyzed molecules. The peak with the highest m/z ratio often represents the molecular ion. The peaks with the lower m/z ratio are the fragment ions.

To quantify the target analyte, we can use three methods: quantitation by external standardization, internal standardization, and isotope dilution. The quantitation by external standardization requires the assembly of the calibration curve of standards. The quantitation by internal standardization is easier and faster. The known amount of a compound with similar ionization efficiency and retention time as the analyte is added to the sample. The quantitation by isotope dilution is a unique form of internal standardization. The compound added to the sample is the analyte labeled by isotope. For example, the methyl in the formula is exchanged for trideuteromethyl. Because the concentration of the standard is known, the concentration of the analyte can be calculated. Sometimes the standards have slightly different time of elution from the chromatography apparatus that separates the mixture before MS (Gross, 2017).

3.3 CHLOROFORM METHANOL EXTRACTION

To identify and quantify lipids from plasma, tissues, cell cultures or exhale breath condensate, they first need to be extracted. In 1928 Bloor published a paper with a new method to extract lipids from plasma and tissues with ethanol-ether mixture, chloroform and petrolether (Bloor, 1928). However, it was replaced by the Folch method to extract the lipids from the brain tissue. The tissue is homogenized in the chloroform-methanol mixture (2:1) (v/v). The sample is filtrated. Because it contains non-lipid substances, it is washed by the water in the volume that represented 20 % of the sample volume. This washing step leads to a loss of nearly a 1 % of extracted brain lipids and to the separation of the two layers. After the extraction the upper layer of methanol and water contains non-lipidic substances and the lover chloroform layer contains nearly all lipids of the brain tissue (Folch, 1957). Nowadays, the filtration step is not often used to avoid contamination. Also, the homogenization of the sample precedes the addition of the extraction mixture if the experiment is performed on microscale samples and the homogenization should be performed in constant low temperatures. When the water is added to the mixture, the composition of the upper layer is 3:48:47 (v/v/v) for chloroform, methanol and water, and the composition of the lower layer is 86:14:1 (v/v/v). Between the layers is interphase with precipitated proteins (Eggers et Schwudke, 2016).

The principle of the Folch method is defined by Nernst's partition law between two non-miscible solvents. The distribution coefficient (K_D) is defined as the concentration of component 1 in solvent A divided by the concentration of component 1 in solvent B. And this coefficient is constant in the given temperature. However, this basic equation does not describe the reality properly due to the tendency of lipids to form micelles and aggregates in all kinds of solvents, polar and non-polar. The Folch method is effective because chloroform/methanol/water mixture has a low capacity for lipid aggregate forming. (Eggers et Schwudke, 2016).

The representation of lipids in the layers is also linked to the presence of mineral salts of Na, K, Ca, and Mg in the sample. The cations of those salts decrease the dissociation of the acidic lipides, which leads to the lipid´s absence in the upper layer (Folch, 1957).

In this thesis, we will use the Folch method to extract the lipids from exhaled breath condensate, which consist mostly of water. And there will be no need to add water in order to separate the layers.

4 MATERIAL AND METHODS

4.1 Biological material

- Exhaled breath condensate from 23 healthy non-smokers aged 20–23

Lipid standards (Avanti Polar Lipids):

- C14 Ceramide (d18:1/14:0) 860514
- C17 Ceramide (d18:1/17:0) 860517
- C18:1 Ceramide (d18:1/18:1(9Z)) 860519
- C18 Ceramide (d18:1/18:0) 860518
- C20 Ceramide (d18:1/20:0) 860520
- C24 Ceramide (d18:1/24:0) 860524
- C24:1 Ceramide (d18:1/24:1(15Z)) 860525
- C16 Ceramide-d7 (d18:1-d7/16:0) 860676
- C18 Ceramide-d7 (d18:1-d7/18:0) 860677
- C18:1 Ceramide-d7 (d18:1-d7/18:1) 860747
- C24 Ceramide-d7 (d18:1-d7/24:0) 860678
- C24:1 Ceramide-d7 (d18:1-d7/24:1(15Z)) 860679

4.2 Chemicals, kits, and solutions

Chemicals

- Chloroform Sigma Aldrich reagents (catalog number: 288306)
- Methanol Sigma Aldrich reagents (catalog number: 322415)
- Ethanol Sigma Aldrich reagents (catalog number: E7023)

Kits

- SecurityGuard 4 × 2.0 mm C18 guard pre-column (Phenomenex)
- Separation column Kinetex 2.1 × 50 mm C18 (Phenomenex)

4.3 Equipment

- Benchtop Centrifuge 5810R (Eppendorf)
- Dionex UltiMate 3000 LC-system (AB sciex)
- Laboratory fume hood (Merci)
- QTrap 5500 mass spectrometers (AB sciex)

- Transportable unit for research of biomarkers obtained and disposable exhaled condensate collection system TURBO DECCS 14 (Medivac)
- Vortex Genius 3 (IKA)

4.4 Methods

Sample collection

Samples were collected from 23 volunteers aged 20 to 23, with normal body mass index and no viral or respiratory diseases. The subjects were non-smokers. Each subject exhaled into the TURBO DECCS apparatus for 10 minutes. TURBO stand for "Transportable Unit for Research of Biomarkers Obtained", and it is a thermoelectric cooling device. DECCS stands for "Disposable Exhaled Condensate Collection System", and it is a set of plastic circuits (Fig. 1). The EBC condensed in – 5 °C. Samples were stored in plastic tubes at – 80 °C (one sample) or processed immediately after their collection (22 samples).

Figure 2 – The TURBO DECCS apparatus. Volunteers exhaled into the plastic tubing, which was equipped with saliva trap, and it led to the opening of the cooling device, where it was connected to the tube inside the cooling chamber.
Medivac.it: https://www.medivac.it/en/turbo-deccs-systems/

Methanol – chloroform extraction

The extraction mixture was prepared from methanol and chloroform (2:1) (v/v). One ml of the extraction mixture was added to each sample. The samples were mixed using the vortex

mixer, centrifuged at 1000 rpm for 10 min and mixed again. Samples were stored in – 4 °C for 1–2 h and centrifuged again at 1000 rpm for 10 min. Then the chloroform fraction with lipids was transported to a separate microtube using the pipette. The chloroform was evaporated using nitrogen. The lipids were resuspended in 50 µl of HPLC pure methanol and then analyzed (Fig. 2).

High-performance liquid chromatography and mass spectrometry

The analysis was performed using a quadrupole QTrap 5500 mass spectrometer. The samples were loaded by the robot to the column automatically. The mobile phases used in liquid chromatography were MilliQ water (A) and methanol (B), both with 0.01% acetic acid. Their gradients were 20 % B in the first minute, increased to 35% in 3 minutes and then increased to 99% in 15 minutes and 100 % in 17 minutes and 6 seconds. After 56 seconds, the B phase decreased to 20 % in one minute, and the column was equilibrated at 20% B for another minute. The run time of the process was 20 minutes. For the MS the conditions were: medium collision gas flow, the drying temperature 400°C, the needle voltage − 4,500 V, the curtain gas 30 psi, the first ion source gas 40 psi and the second ion source gas 30 psi.

Analysis of the samples and calculations

Each sample was analyzed five times to ascertain the highest level of analysis and lower statistical error; the standard deviation was not above 10 % of the mean. A standard curve was performed for each ceramide and ergosterol. The standard curves were performed between 1 fg/µl up to 5000 fg/µl. All the standard curves had a good correlation, $\geq$ 0,9. The standard curves are included in the appendix (Graphs 7 – 17).

For ergosterol values, the positiveness criteria were to detect quantifiable ergosterol in at least 3 of the 5 analyses with a standard deviation not above 10 % of the mean. None of the negative samples had detectable ergosterol values in the five readings, and consequently, they were labelled as negative.

Statistical analysis

The paired and unpaired Student's t-test was used to compare different groups. Also, the Person coefficient was used to calculate correlations among the values of the diverse species analyzed.

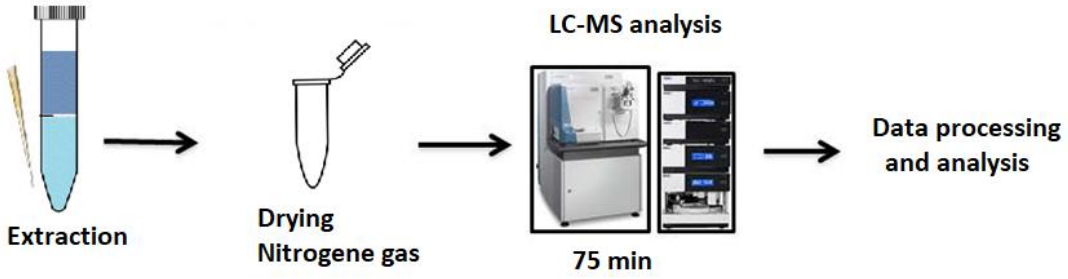

Figure 3 – The analysis schema. The chloroform-methanol extraction was followed by drying of the lipid layer with nitrogen. Resuspended lipids were analyzed using LC-MS.

5 RESULTS

The analysis was performed on ceramides C14:0, C16:0, C17:0, C18:1, C20:0, C22:0, C24:1, C26:0 and ergosterol. The values of the ceramides and ergosterol are in Table 1. And they are also captured in Graph 1. Correlations between individual ceramides in the complete analysis are in Table 2. The ergosterol was detected in 15 of the 23 samples. The ergosterol levels in the 8 remaining samples were under detection limit (Tab. 3) (Tab. 4). We found higher levels of ceramide C24:1 in the ergosterol positive samples than the negative ergosterol samples, P = 0,037707 (Tab. 4) (Graph 2). And we also detected elevated levels of ceramide C26:0 in the ergosterol negative samples compared to the ergosterol positive samples (Tab. 4) (Graph 2). The P-value was 0,038853 (Tab.4).

Correlations between individual ceramides in the samples without detectable ergosterol are in Table 5. Correlations between individual ceramides in the samples with detectable ergosterol are in Table 6.

We also compared the levels of ceramide in the group of samples with ergosterol levels lower than 5 pmol (Tab. 7) and in the group of samples with ergosterol levels higher than 5 pmol (Tab. 8). The significant P-value 0,026206 was calculated for ceramide C16:0 (Graph 3). The levels of ceramides were also compared between sexes and significant P value 0,0004 was observed in the ceramide C18:1, which was elevated in females and in ceramide C24:1 (P value 0,04) which was elevated in males (Graph 4).

The levels of ceramide originating from long-chain fatty acids and very long-chain fatty acids were compared in graph 5. However, they did not display significant differences. The levels of ceramide originating from long-chain fatty acids and very long-chain fatty acids were also compared between sexes (Graph 6).

Table 1 – The ceramides and ergosterol values in each sample of the collected EBC analyzed by HPLCMS.

	Analyte [pmol]										
SN	C14	C16	C17	C18	C18:1	C20	C22	C24	C24:1	C26:0	Ergosterol
1	7,50718	8,357897	8,211543	10,29989	12,77042	8,233206	8,896045	16,70759	10,91085	8,105381	0,29
2	8,134704	12,42564	9,416145	3,374457	6,69802	5,115751	7,106715	14,0843	27,29656	6,347708	1,8748684
3	6,834116	13,16629	6,620469	8,915932	7,381708	11,93502	1,081217	13,91584	24,48262	5,666788	3,4477143
4	4,392188	8,145975	6,055388	13,24203	10,51473	24,29081	4,865457	14,30621	13,07682	1,110386	1,8747161
5	8,718131	6,906467	2,019519	16,23549	16,27075	12,82303	20,30441	8,005647	5,062965	3,65359	8,7490894
6	2,687682	6,858826	1,771493	12,86449	15,09433	14,10746	15,20056	6,865605	7,999894	16,54965	0
7	2,684777	7,216352	3,618259	15,58099	17,05733	16,00612	17,25435	8,951662	7,554442	4,075717	5,8214801
8	4,617863	7,565679	0,94159	8,16364	14,72596	13,04769	13,97864	4,820583	15,61386	16,5245	0
9	6,189561	8,464337	0,042436	9,873646	17,08768	9,546614	18,18466	4,395964	11,73521	14,47989	3,5121127
10	3,302716	8,411092	1,28671	7,51761	16,49296	11,90555	17,56353	6,394213	5,080803	22,04482	0
11	8,698664	3,649188	0,516674	12,309	11,20837	10,15441	22,61184	6,945636	6,799455	17,10675	3,7856166
12	10,18562	3,916657	0,740646	11,50459	14,01284	12,04891	14,20461	5,127651	7,359	20,89947	5,1868652
13	11,62631	3,826889	0,899278	9,401569	16,62703	9,125186	14,32916	4,962807	9,710059	19,49171	0
14	3,331384	5,955782	3,641249	17,16259	18,48664	13,03029	19,19855	8,540228	7,665575	2,987713	0
15	8,091564	6,381498	6,248023	5,76854	13,20199	8,408998	10,58481	9,772488	18,02603	13,51606	4,688183
16	11,71964	5,570657	9,721993	7,889872	14,23702	6,168309	14,42852	3,006354	8,893488	18,36414	0
17	13,0186	4,753413	5,326765	11,06636	12,69829	10,59126	13,2256	5,20225	4,562414	19,55504	0
18	6,857707	6,705917	0,590752	6,568038	15,98429	8,513996	14,39118	6,541999	14,25292	19,5932	2,1794434
19	10,96579	7,423202	6,920699	10,50367	6,659362	8,000124	14,2627	4,817257	13,7464	16,70079	5,6251339
20	4,7567017	4,700449	3,663621	7,441345	11,09874	7,920273	14,21968	14,62305	9,278161	7,997983	7,8117634
21	5,8836476	3,807139	6,579434	10,58551	6,751311	4,188086	13,6578	15,21719	12,34977	6,680116	0
22	5,9142248	3,965356	6,642125	9,258651	12,49747	3,706999	10,50582	9,143807	16,2721	7,793454	8,5349197
23	7,9360128	4,027267	0,601657	6,922421	13,31793	4,712794	7,979444	11,43601	19,3536	9,412861	11,249196

SN stands for sample number.

Table 2 – The Person's correlation coefficient for different types of ceramides in all 23 analyzed samples of EBC.

Ceramide	C14	C16	C17	C18	C18:1	C20	C22	C24	C24:1
C14									
C16	- 0,3205								
C17	0,190101	0,307135							
C18	-0,2611	-0,31223	-0,18377						
C18:1	-0,26227	-0,38978	-0,61694	0,291349					
C20	-0,47416	0,170071	-0,28031	0,509732	0,17445				
C22	-0,11589	-0,49848	-0,50499	0,458729	0,526617	-0,04104			
C24	-0,26077	0,25034	0,445377	-0,05045	-0,44435	-0,08518	-0,47486		
C24:1	0,019612	0,503481	0,370817	-0,57647	-0,51503	-0,37614	-0,71236	0,475264	
C26:0	0,392472	-0,35285	-0,38162	-0,41751	0,183223	-0,27523	0,271825	-0,68112	-0,30741

The significant correlations are highlighted.

Table 3 – The values of ceramides in samples without detectable ergosterol with their mean value and standard deviation.

	Analyte [pmol]										
SN	C14	C16	C17	C18	C18:1	C20	C22	C24	C24:1	C26:0	Ergosterol
6	2,687682	6,858826	1,771493	12,86449	15,09433	14,10746	15,20056	6,865605	7,999894	16,54965	0
8	4,617863	7,565679	0,94159	8,16364	14,72596	13,04769	13,97864	4,820583	15,61386	16,5245	0
10	3,302716	8,411092	1,28671	7,51761	16,49296	11,90555	17,56353	6,394213	5,080803	22,04482	0
13	11,62631	3,826889	0,899278	9,401569	16,62703	9,125186	14,32916	4,962807	9,710059	19,49171	0
14	3,331384	5,955782	3,641249	17,16259	18,48664	13,03029	19,19855	8,540228	7,665575	8,963139	0
16	11,71964	5,570657	9,721993	7,889872	14,23702	6,168309	14,42852	3,006354	8,893488	18,36414	0
17	13,0186	4,753413	5,326765	11,06636	12,69829	10,59126	13,2256	5,20225	4,562414	19,55504	0
21	5,8836476	3,807139	6,579434	10,58551	6,751311	4,188086	13,6578	15,21719	12,34977	6,680116	0
Mean	7,02348	5,843685	3,771064	10,58145	14,38919	10,27048	15,1978	6,876154	8,984482	16,02164	
SD	4,351395	1,693607	3,210717	3,221101	3,546689	3,54488	2,094091	3,746199	3,651044	5,397228	

SN stands for sample number.

Table 4 – The values of ceramides in samples with detectable ergosterol with their mean value and standard deviation and with P-values comparing the ceramide values of these samples to the ceramide values of the samples without detectable ergosterol.

	Analyte [pmol]										
SN	C14	C16	C17	C18	C18:1	C20	C22	C24	C24:1	C26:0	Ergosterol
1	7,50718	8,357897	8,211543	10,29989	12,77042	8,233206	8,896045	16,70759	10,91085	8,105381	0,29
2	8,134704	12,42564	9,416145	3,374457	6,69802	5,115751	7,106715	14,0843	27,29656	6,347708	1,874868
3	6,834116	13,16629	6,620469	8,915932	7,381708	11,93502	1,081217	13,91584	24,48262	5,666788	3,447714
4	4,392188	8,145975	6,055388	13,24203	10,51473	24,29081	4,865457	14,30621	13,07682	1,110386	1,874716
5	8,718131	6,906467	2,019519	16,23549	16,27075	12,82303	20,30441	8,005647	5,062965	3,65359	8,749089
7	2,684777	7,216352	3,618259	15,58099	17,05733	16,00612	17,25435	8,951662	7,554442	4,075717	5,82148
9	6,189561	8,464337	0,042436	9,873646	17,08768	9,546614	18,18466	6,593946	11,73521	14,47989	3,512113
11	8,698664	3,649188	0,516674	12,309	11,20837	10,15441	22,61184	6,945636	6,799455	17,10675	3,785617
12	10,18562	3,916657	0,740646	11,50459	14,01284	12,04891	14,20461	5,127651	7,359	20,89947	5,186865
15	8,091564	6,381498	6,248023	5,76854	13,20199	8,408998	10,58481	9,772488	18,02603	13,51606	4,688183
18	6,857707	6,705917	0,590752	6,568038	15,98429	8,513996	14,39118	6,541999	14,25292	19,5932	2,179443
19	10,96579	7,423202	6,920699	10,50367	6,659362	8,000124	14,2627	4,817257	13,7464	16,70079	5,625134
20	4,756702	4,700449	3,663621	7,441345	11,09874	7,920273	14,21968	14,62305	9,278161	7,997983	7,811763
22	5,914225	3,965356	6,642125	9,258651	12,49747	3,706999	10,50582	9,143807	16,2721	7,793454	8,53492
23	7,936013	4,027267	0,601657	6,922421	13,31793	4,712794	7,979444	11,43601	19,3536	9,412861	11,2492
Mean	7,191129	7,030166133	4,127197	9,853246	12,38411	10,09447	12,4302	10,06487	13,68048	10,43067	4,975407
SD	2,115266	2,799062335	3,101156	3,459246	3,396499	4,925486	5,71187	3,726232	6,274285	5,973334	2,949238942
P-value	0,920788	0,229493684	0,803556	0,626407	0,21576	0,923858	0,119108	0,073783	0,037707	0,038853	0,00001916

SN stands for sample number. Significant P-values are highlighted.

Table 5 – The Person's correlation coefficient for different types of ceramides in the samples of EBC without detectable ergosterol.

Ceramide	C14	C16	C17	C18	C18:1	C20	C22	C24	C24:1
C14									
C16	-0,73319								
C17	0,475355	-0,43536							
C18	-0,32831	-0,24567	0,049537						
C18:1	-0,27263	0,378511	-0,57786	0,088113					
C20	-0,60022	0,62912	-0,77478	0,232754	0,670861				
C22	-0,66543	0,326254	-0,11684	0,541606	0,384718	0,229026			
C24	-0,27733	-0,26053	0,267602	0,456598	-0,65276	-0,39979	0,362383		
C24:1	-0,14091	-0,09303	0,047835	-0,09407	-0,43194	-0,28321	-0,19686	0,399048	
C26:0	0,363459	0,215825	-0,24402	-0,83871	0,105206	0,061631	-0,59617	-0,64403	-0,32935

Significant correlations are highlighted.

Table 6 – The Person's correlation coefficient for different types of ceramides and ergosterol in the samples of EBC with detectable ergosterol.

Analyte	C14	C16	C17	C18	C18:1	C20	C22	C24	C24:1	C26:0
C14										
C16	-0,216270683									
C17	-0,083767045	0,536538								
C18	-0,227926347	-0,32105	-0,29129							
C18:1	-0,288068533	-0,54487	-0,64631	0,356605						
C20	-0,501350914	0,088719	-0,11347	0,607352	0,031074					
C22	0,088163307	-0,62491	-0,61976	0,437774	0,523219	-0,08801				
C24	-0,337568055	0,326802	0,556429	-0,25593	-0,28236	0,021752	-0,6014			
C24:1	-0,337568055	0,540172	0,503053	-0,75618	-0,48504	-0,4319	-0,75489	0,411114		
C26:0	0,187819918	-0,46883	-0,47463	-0,30815	0,108139	-0,44478	0,403233	-0,63374	-0,15151	
Ergosterol	0,187819918	-0,51801	-0,29487	0,235092	0,374451	-0,25637	0,298681	-0,06073	-0,02764	-0,040195381

The significant correlations are highlighted.

Table 7 – The values of ceramides and ergosterol in the samples with detectable ceramides levels lower than 5 pmol.

	Analyte [pmol]										
SN	C14	C16	C17	C18	C18:1	C20	C22	C24	C24:1	C26:0	Ergosterol
1	7,50718	8,357897	8,211543	10,29989	12,77042	8,233206	8,896045	16,70759	10,91085	8,105381	0,29
2	8,134704	12,42564	9,416145	3,374457	6,69802	5,115751	7,106715	14,0843	27,29656	6,347708	1,874868
3	6,834116	13,16629	6,620469	8,915932	7,381708	11,93502	1,081217	13,91584	24,48262	5,666788	3,447714
4	4,392188	8,145975	6,055388	13,24203	10,51473	24,29081	4,865457	14,30621	13,07682	1,110386	1,874716
9	6,189561	8,464337	0,042436	9,873646	17,08768	9,546614	18,18466	6,593946	11,73521	14,47989	3,512113
11	8,698664	4,649188	0,516674	12,309	11,20837	10,15441	22,61184	6,945636	6,799455	17,10675	3,785617
15	8,091564	6,381498	6,248023	5,76854	13,20199	8,408998	10,58481	9,772488	18,02603	13,51606	4,688183
18	6,857707	6,705917	0,590752	6,568038	15,98429	8,513996	14,39118	6,541999	14,25292	19,5932	2,179443
Mean	7,0882105	8,537093	4,712679	8,793942	11,8559	10,77485	10,96524	11,1085	15,82256	10,74077	2,7065818
SD	1,3661608	2,924191	3,752568	3,360871	3,70142	5,7955	7,108508	4,117215	7,007702	6,384225	1,403603

SN stands for sample number

Table 8 – The values of ceramides and ergosterol in the samples with detectable ceramides levels higher than 5 pmol and the P-value comparing the ceramide values in samples with ergosterol levels under 5 pmol and over 5 pmol.

	Analyte [pmol]										
S.N.	C14	C16	C17	C18	C18:1	C20	C22	C24	C24:1	C26:0	Ergosterol
5	8,718131	6,906467	2,019519	16,23549	16,27075	12,82303	20,30441	8,005647	5,062965	3,65359	8,749089
7	2,684777	7,216352	3,618259	15,58099	17,05733	16,00612	17,25435	8,951662	7,554442	4,075717	5,82148
12	10,18562	3,916657	0,740646	11,50459	14,01284	12,04891	14,20461	5,127651	7,359	20,89947	5,186865
19	10,96579	7,423202	6,920699	10,50367	6,659362	8,000124	14,2627	4,817257	13,7464	16,70079	5,625134
20	4,756702	4,700449	3,663621	7,441345	11,09874	7,920273	14,21968	14,62305	9,278161	7,997983	7,811763
22	5,914225	3,965356	6,642125	9,258651	12,49747	3,706999	10,50582	9,143807	16,2721	7,793454	8,53492
23	7,936013	4,027267	0,601657	6,922421	13,31793	4,712794	7,979444	11,43601	19,3536	9,412861	11,2492
Mean	7,308751143	5,450821	3,458075	11,06388	12,98777	9,316893	14,10443	8,872155	11,23238	10,07626643	7,56835
SD	2,99635644	1,398299	2,815823	3,164748	3,470992	4,206375	3,567011	4,386512	6,483784	5,78700966	2,176978
P-value	0,862213211	0,026206	0,460106	0,237661	0,552006	0,593029	0,308534	0,272473	0,173528	0,844412302	0,000489

SN stands for sample number

Graph 1 – The graph of complete analysis of the 23 collected EBC samples for ceramides and ergosterol.

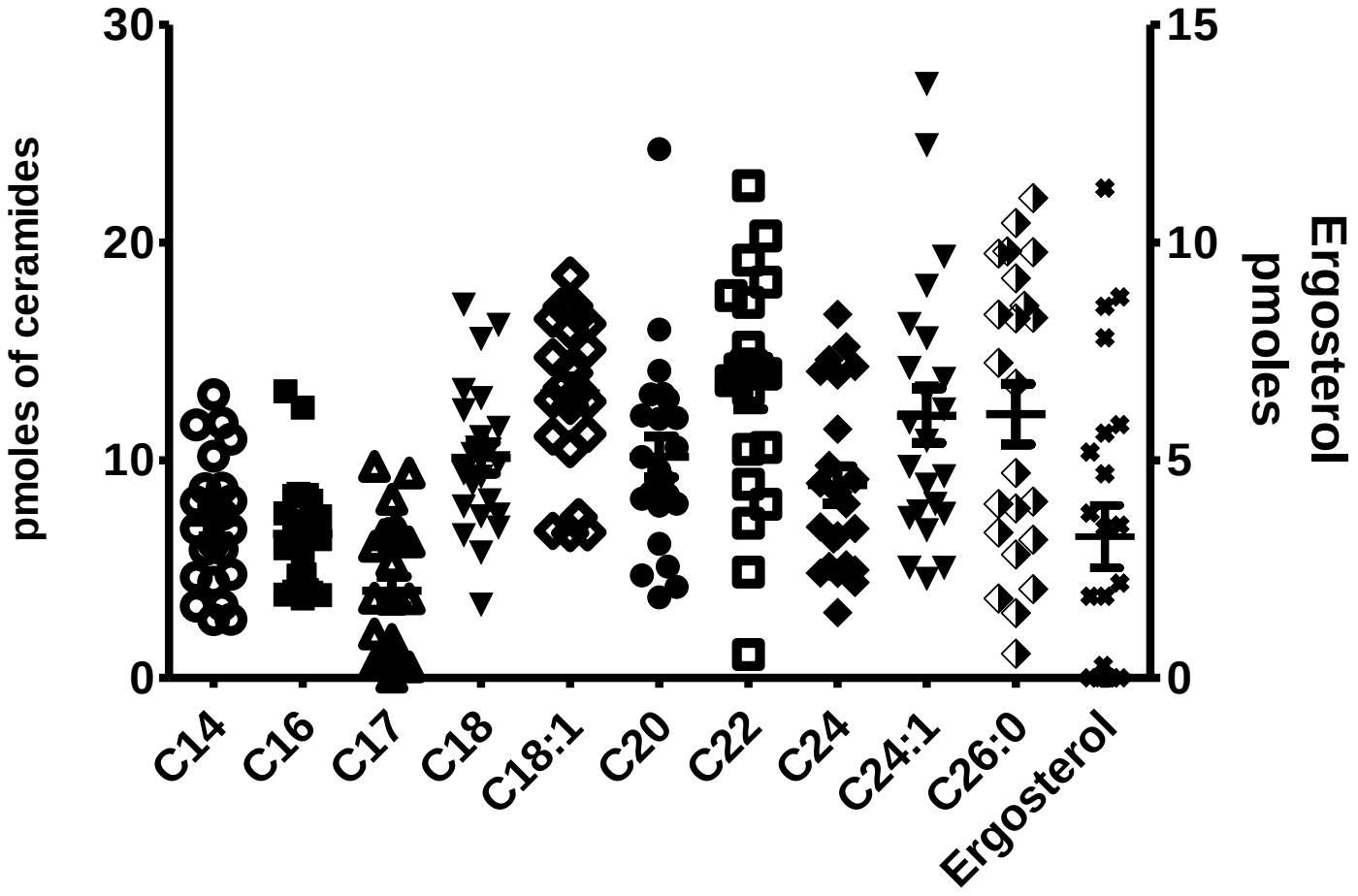

The left y-axis is reference axis for ceramides values. The right y-axis is reference axis for ergosterol due to its lower levels.

Graph 2 –The differences in ceramides levels in the EBC samples with and without detectable ergosterol

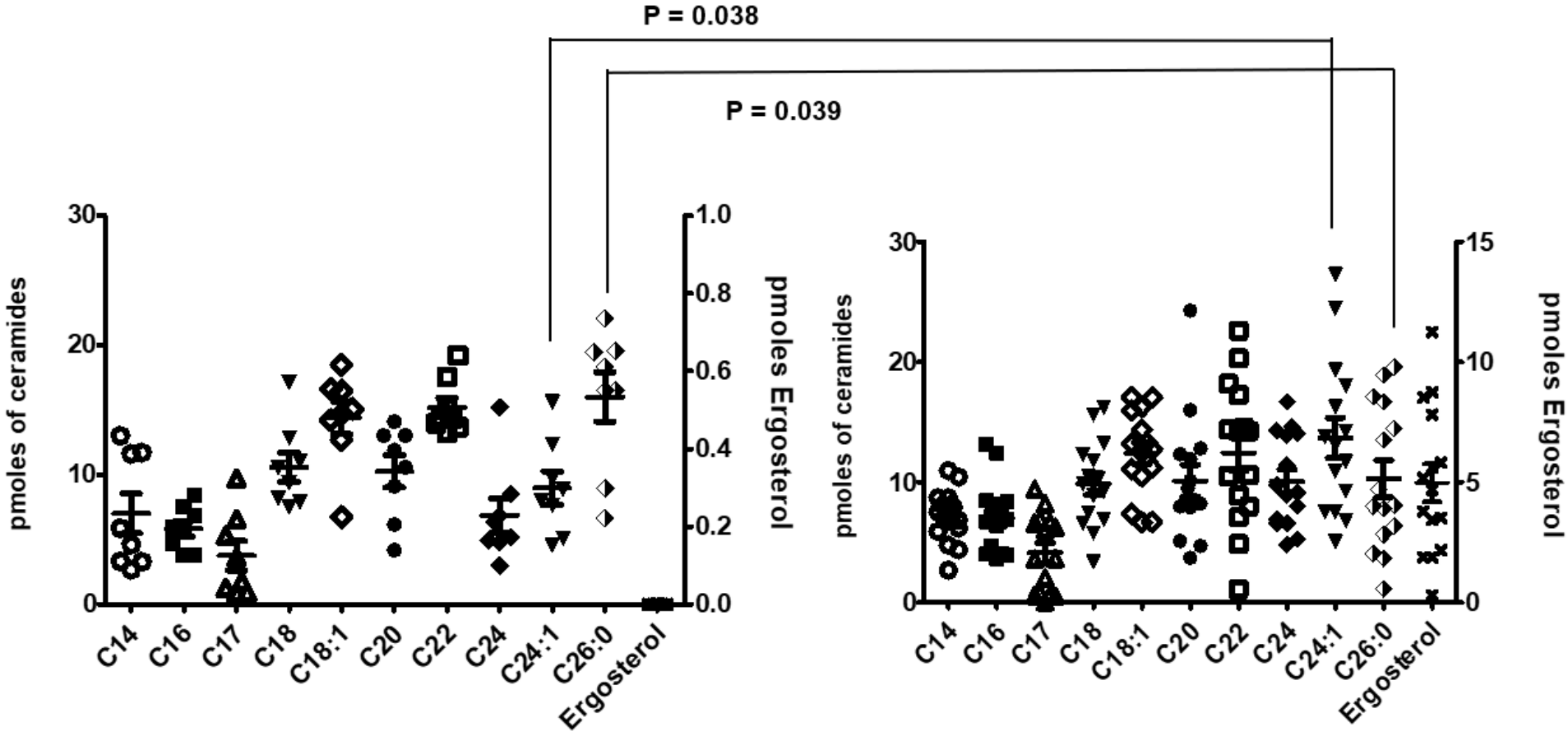

P stands for P-value. The left y-axes are reference axes for ceramides values. The right y-axes are reference axes for ergosterol due to its lower levels. Significant differences were observed in the C24:1 and C26 ceramide values.

Graph 3 – The differences in ceramides levels in the samples with ergosterol levels under 5 pmol and over 5 pmol.

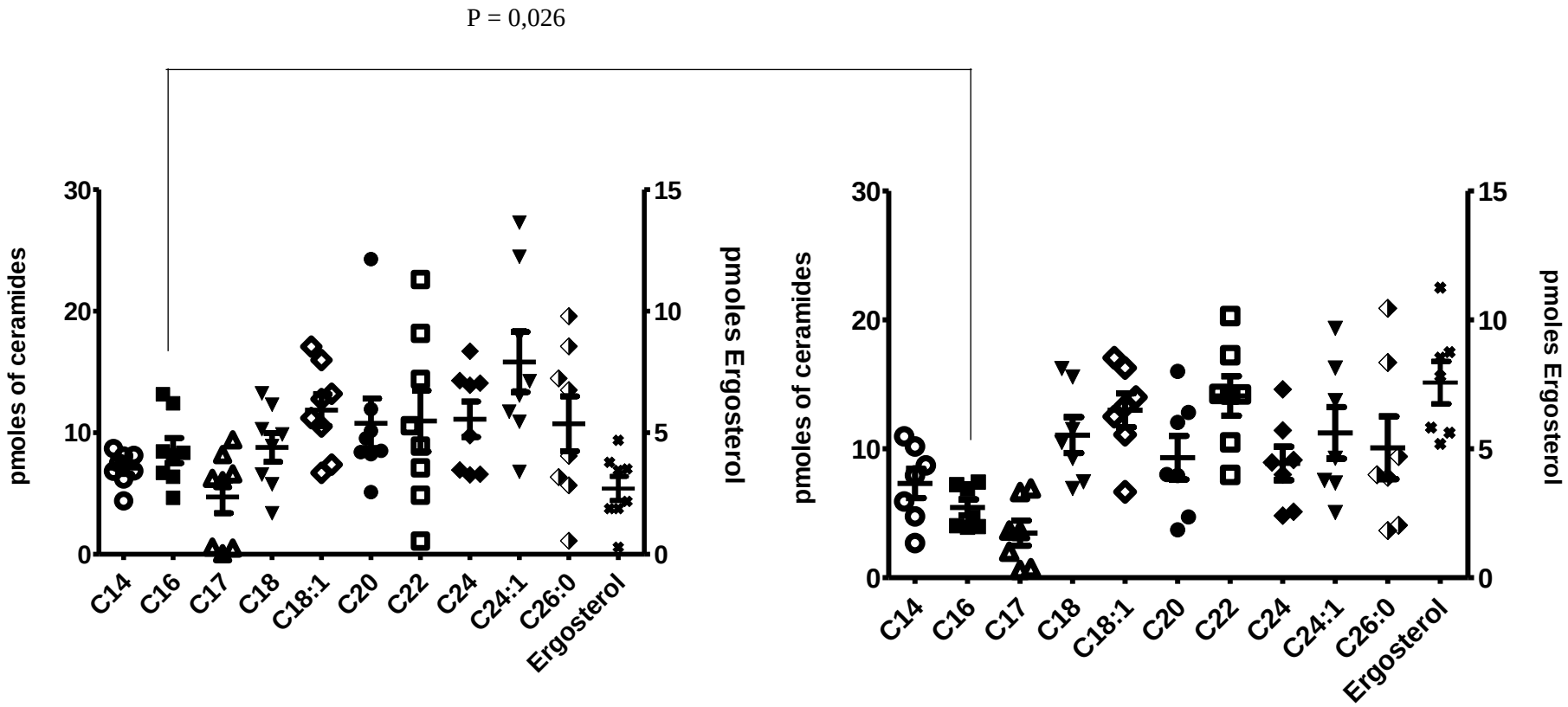

P stands for P-value. The left y-axes are reference axes for ceramides values. The right y-axes are reference axes for ergosterol due to its lower levels. Significant difference was observed in the C16 ceramide values.

Graph 4 – The comparison of values of ceramides and ergosterol in males and females.

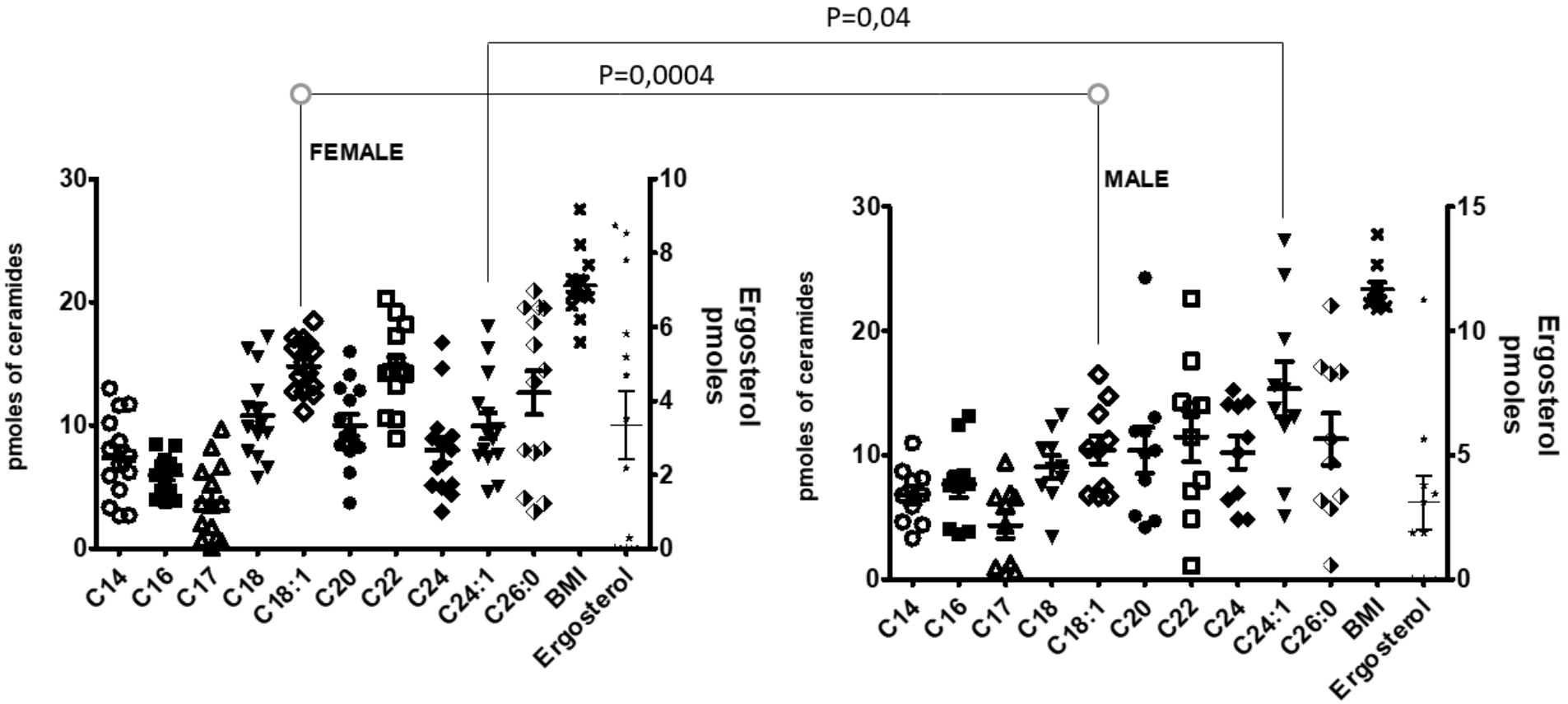

P stands for P-value. The left y-axes are reference axes for ceramides values. The right y-axes are reference axes for ergosterol due to its lower levels. Significant differences were observed in the C18:1 and C24:1 ceramide values.

Graph 5 – The levels of ceramides with long-chain fatty acids and ceramides with very-long-chain fatty acids in the samples of EBC with and without detectable ergosterol. No significant differences were encountered.

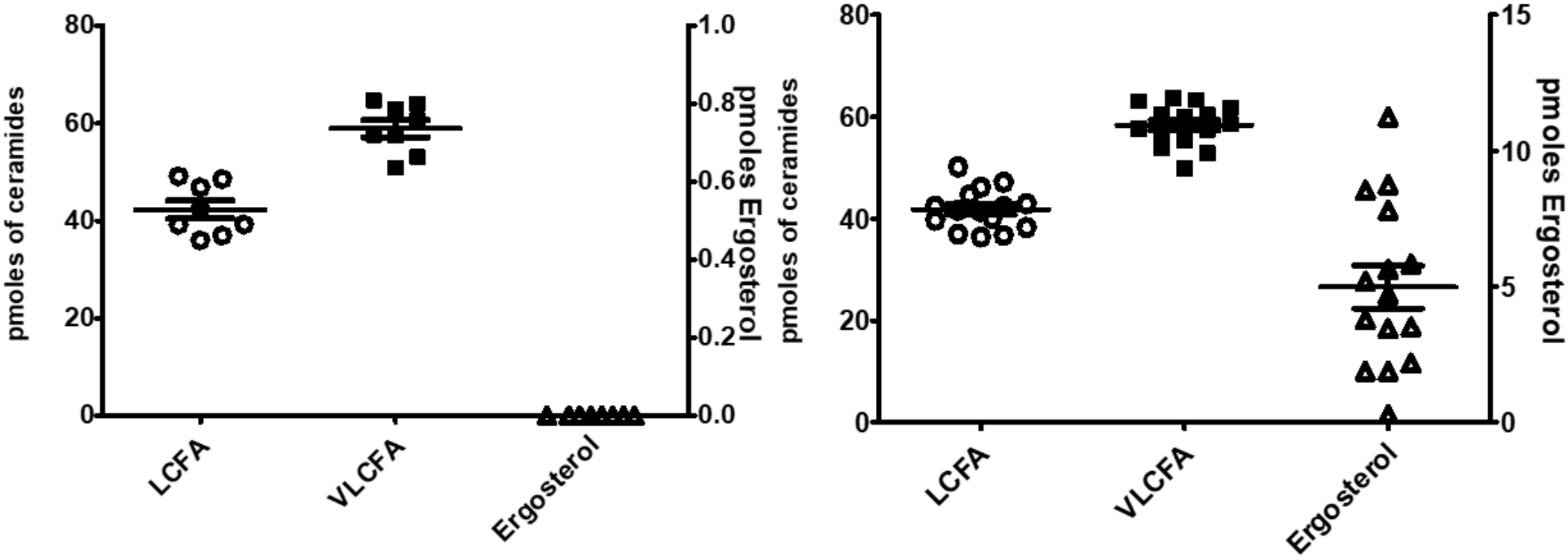

LCFA stands for long chain fatty acid ceramides. VLCFA stands for very long chain fatty acid ceramides. The left y-axes are reference axes for ceramides values. The right y-axes are reference axes for ergosterol due to its lower levels

Graph 6 – The comparison of the levels of ceramides with long chain and very long chain fatty acids in EBC samples of males and females.

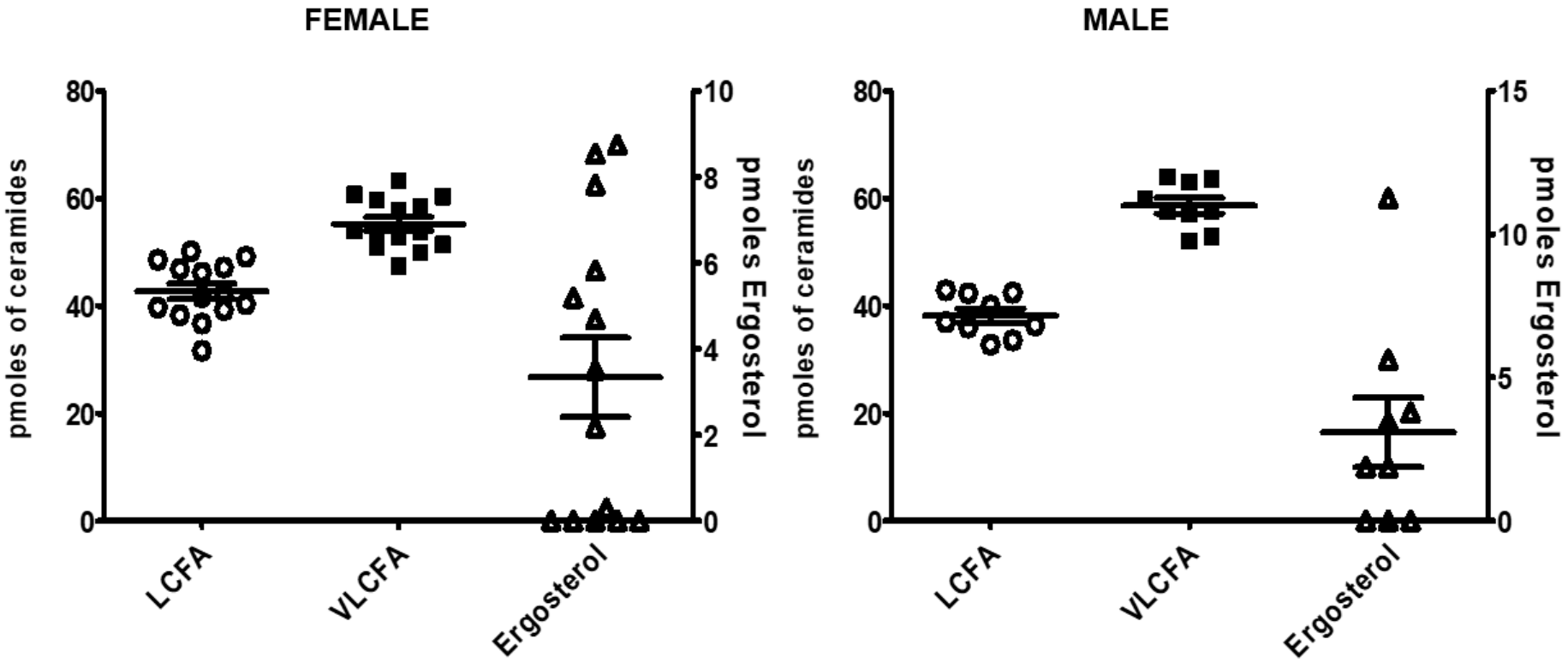

LCFA stands for long chain fatty acid ceramides. VLCFA stands for very long chain fatty acids ceramides. The left y-axes are reference axes for ceramides values. The right y-axes are reference axes for ergosterol due to its lower levels.

6 DISCUSSION

Even though nitro oxide detection in the exhaled breath by specific apparatus FeNO is generally accepted as an excellent clinical marker of the airways' inflammation, there are still limitations on the analysis. These limitations are because nitric oxide production in the upper airways is higher than in the lower airways. (Turner et al.,2019)

Exhaled breath condensate is a non-invasive, simple technique that may identify different metabolites involved in the airways' inflammation. Most of the research has been devoted to the analysis of cytokines or leukotrienes, prostaglandin metabolites. However, little is known about other inflammatory markers.

In recent years, ceramides have been considered essential biomarkers of respiratory diseases (Garić et al., 2019) (Garić et al.,2020). Interestingly, there have been no reports of these lipid moieties in the exhaled breath condensate. We aimed to analyse ceramide species as critical biomarkers of the airways' inflammation.

Rhinitis is defined as irritation and inflammation of the mucous membrane inside the nose. It has been linked to infections of *Aspergillus, Alternaria, Candida, Cladosporium* and *Penicillium* species (DeShazo et al. 1997) (Stammberger et al., 1984) (Ponikau et al. 1999). The fungi in the airways may form a biofilm and then raise the host's IgE levels and cause chronic inflammation (Foreman et al., 2012). Although immunocompromised or older adults are at a higher risk of fungi infections, they are not uncommon in a relatively healthy population. Fungi spores are also prevalent in the environment. Sometimes their levels are even higher than pollen levels, and they can impact upper airways, for example, when the subject is exposed to the moulds (Bush et Yunginger, 1987).

We hypothesized that ceramide levels would be increased in individuals with elevated ergosterol, a sterol found in fungi cell membranes, compared to controls (Petrache et al., 2013). We found a positive correlation between ceramide C24:1 and ergosterol and a negative correlation between ceramide C26:0 and ergosterol. These results suggest that ergosterol may be a critical biomarker for fungi derived subclinical inflammation. Individual ceramides also correlated with each other. However, the correlations were more significant in the samples that lack ergosterol.

When we divided the samples with positive ergosterol into two groups, lower and higher than 5 pmols, a significant difference was observed. There were higher levels of ceramide C16:0 in the group with low ergosterol levels. Even though the significance of this finding

has to be confirmed in a higher amount of samples, it suggests that changes in other ceramides species is also possible.

Gender seems to be important in the amount of detectable C18:1 and C24:1 species; however, caution should be taken since ergosterol levels were higher in female than in male donors. As expressed before, C24:1 levels differ between the groups lacking ergosterol to those with detectable ergosterol.

In general, ceramide levels are essential markers in exhaled breath condensate as well as ergosterol. Extension of the studied data set and evaluation of the tested subject's mycobiome is needed to analyze this topic further to confirm our hypothesis.

7 CONCLUSION

1. Ceramides are essential biomarkers in lung physiology and can be detected in exhaled breath condensate.
2. There are gender differences in ceramide species that may be relevant for lung physiology.
3. Ergosterol is a potential biomarker linked to airway inflammation caused by fungi.

8 REFERENCES

AUG, Argo, Siiri ALTRAJA, Kalle KILK, Rando POROSK, Ursel SOOMETS, Alan ALTRAJA and Marco IDZKO. E-Cigarette Affects the Metabolome of Primary Normal Human Bronchial Epithelial Cells. *PLOS ONE* [online]. 2015, **10**(11) [cit. 2021-03-11]. ISSN 1932-6203. Doi: 10.1371/journal.pone.0142053

AREVALO, Ricardo, Ziqin NI and Ryan M. DANELL. Mass spectrometry and planetary exploration: A brief review and future projection. *Journal of Mass Spectrometry* [online]. 2020, **55**(1) [cit. 2021-03-19]. ISSN 1076-5174. Doi:10.1002/jms.4454

AVOTA, Elita, Erich GULBINS, Sibylle SCHNEIDER-SCHAULIES and John A. T. YOUNG. DC-SIGN Mediated Sphingomyelinase-Activation and Ceramide Generation Is Essential for Enhancement of Viral Uptake in Dendritic Cells. *PLoS Pathogens* [online]. 2011, **7**(2) [cit. 2021-03-14]. ISSN 1553-7374. Doi:10.1371/journal.ppat.1001290

BALAZY, Michael. Eicosanomics: targeted lipidomics of eicosanoids in biological systems. *Prostaglandins & Other Lipid Mediators* [online]. 2004, **73**(3-4), 173-180 [cit. 2021-03-17]. ISSN 10988823. Doi:10.1016/j.prostaglandins.2004.03.003

BANNIER, Michiel A. G. E., Philippe P. R. ROSIAS, Quirijn JÖBSIS a Edward DOMPELING. Exhaled Breath Condensate in Childhood Asthma: A Review and Current Perspective. *Frontiers in Pediatrics* [online]. 2019,7[cit. 2020-04-23]. DOI: 10.3389/fped.2019.00150.

BENLIMAME, Naciba, Phuong U. LE and Ivan R. NABI. Localization of Autocrine Motility Factor Receptor to Caveolae and Clathrin-independent Internalization of Its Ligand to Smooth Endoplasmic Reticulum. *Molecular Biology of the Cell* [online]. 1998, **9**(7), 1773-1786 [cit. 2021-03-20]. ISSN 1059-1524. Doi:10.1091/mbc.9.7.1773

BERNARD, Dominique, Anne-Marie MINONDO, Christiane CAMUS, Françoise FIAT, Pierre CORCUFF, Rainer SCHMIDT, Michel SIMON and Guy SERRE. Persistence of Both Peripheral and Non-Peripheral Corneodesmosomes in the Upper Stratum Corneum of Winter Xerosis Skin Versus only Peripheral in Normal Skin. *Journal of Investigative Dermatology* [online]. 2001, **116**(1), 23-30 [cit. 2021-03-07]. ISSN 0022202X. Doi:10.1046/j.1523-1747.2001.00208.x

BLOOR, W.R. The determination of small amounts of lipid in blood plasma. *Journal of Biological Chemistry* [online]. 1928, **77**(1), 53-73 [cit. 2021-03-19]. ISSN 00219258. Doi:10.1016/S0021-9258(18)84041-8

BROWN, Deborah A. and John K. ROSE. Sorting of GPI-anchored proteins to glykolipid-enriched membrane subdomains during transport to the apical cell surface. *Cell* [online]. 1992, **68**(3), 533-544 [cit. 2021-03-10]. ISSN 00928674. Doi:10.1016/0092-8674(92)90189-J

BOCK, Jürgen and Erich GULBINS. The transmembranous domain of CD40 determines CD40 partitioning into lipid rafts. *FEBS Letters* [online]. 2003, **534**(1-3), 169-174 [cit. 2021-03-14]. ISSN 00145793. Doi:10.1016/S0014-5793(02)03784-5

BOURBON, Nicole A., Jong YUN and Mark KESTER. Ceramide Directly Activates Protein Kinase Cζ to Regulate a Stress-activated Protein Kinase Signaling Complex. *Journal of Biological Chemistry* [online]. 2000, **275**(45), 35617-35623 [cit. 2021-03-07]. ISSN 00219258. Doi:10.1074/jbc.M007346200

BOWLER, Russell P., Sean JACOBSON, Charmion CRUICKSHANK, et al. Plasma Sphingolipids Associated with Chronic Obstructive Pulmonary Disease Phenotypes. *American Journal of Respiratory and Critical Care Medicine* [online]. 2015, **191**(3), 275-284 [cit. 2021-03-11]. ISSN 1073-449X. Doi:10.1164/rccm.201410-1771OC

BUSH, R.K., YUNGINGER, J.W. Standardization of fungal allergens. Clinical Reviews In Allergy 5, 3–21 (1987). Doi: .org/10.1007/BF02802254

CASTILLO, S. Sianna, Michal LEVY, Chunbo WANG, Jyoti V. THAIKOOTTATHIL, Elaine KHAN and Tzipora GOLDKORN. Nitric oxide-enhanced caspase-3 and acidic sphingomyelinase interaction: A novel mechanism by which airway epithelial cells escape ceramide-induced apoptosis. Experimental Cell Research [online]. 2007, 313(4), 816-823 [cit. 2021-03-13]. ISSN 00144827. Doi:10.1016/j.yexcr.2006.12.001

CRUICKSHANK-QUINN, Charmion, Michael ARMSTRONG, Roger POWELL, Joe GOMEZ, Marc ELIE a Nichole REISDORPH. Determining the presence of asthma-related molecules and salivary contamination in exhaled breath condensate. *Respiratory Research* [online]. 2017, 18(1) [cit. 2020-04-23]. DOI: 10.1186/s12931-017-0538-5. ISSN 1465-993X.

CUELLAR, T. L., T. H. DAVIS, P. T. NELSON, G. B. LOEB, B. D. HARFE, E. ULLIAN and M. T. MCMANUS. Dicer loss in striatal neurons produces behavioral and neuroanatomical phenotypes in the absence of neurodegeneration. *Proceedings of the National Academy of Sciences* [online]. 2008, **105**(14), 5614-5619 [cit. 2021-03-08]. ISSN 0027-8424. Doi:10.1073/pnas.0801689105

COSSART, P., VICENTE, M.F., MENGAUD, J., BAQUERO, F., PEREZ-DIAZ, J.C., and BERCHE. Listeriolysin O is essential for virulence of Listeria monocytogenes: direct evidence obtained by gene complementation. Infection and Immunity. 1989, 57(11). [cit. 2021-03-08] 3629–3636.

EBEL, Philipp, Silke IMGRUND, Katharina VOM DORP, et al. Ceramide synthase 4 deficiency in mice causes lipid alterations in sebum and results in alopecia. *Biochemical Journal* [online]. 2014, **461**(1), 147-158 [cit. 2021-03-20]. ISSN 0264-6021. Doi:10.1042/BJ20131242

EBEL, Philipp, Katharina VOM DORP, Elisabeth PETRASCH-PARWEZ, et al. Inactivation of Ceramide Synthase 6 in Mice Results in an Altered Sphingolipid Metabolism and Behavioral Abnormalities. *Journal of Biological Chemistry* [online]. 2013, **288**(29), 21433-21447 [cit. 2021-03-08]. ISSN 00219258. Doi:10.1074/jbc.M113.479907

EGGERS, Lars F. a Dominik SCHWUDKE. Liquid Extraction: Folch. WENK, Markus R., ed. *Encyclopedia of Lipidomics* [online]. Dordrecht: Springer Netherlands, 2016, 2016-5-11, s. 1-6 [cit. 2021-03-19]. ISBN 978-94-007-7864-1.Doi:10.1007/978-94-007-7864-1_89-1

EL-ANEED, Anas, Aljandro COHEN and Joseph BANOUB. Mass Spectrometry, Review of the Basics: Electrospray, MALDI, and Commonly Used Mass Analyzers. *Applied Spectroscopy Reviews* [online]. 2009, **44**(3), 210-230 [cit. 2021-03-19]. ISSN 0570-4928. Doi:10.1080/05704920902717872

ENARI, Masato, Hideki SAKAHIRA, Hideki YOKOYAMA, Katsuya OKAWA, Akihiro IWAMATSU and Shigekazu NAGATA. A caspase-activated DNase that degrades DNA during apoptosis, and its inhibitor ICAD. *Nature* [online]. 1998, **391**(6662), 43-50 [cit. 2021-03-13]. ISSN 0028-0836. Doi:10.1038/34112

FOLCH J, LEES M, SLOANE STANLEY GH. A simple method for the isolation and purification of total lipides from animal tissues. J Biol Chem. 1957 May;226(1):497-509. PMID: 13428781.

FOREMAN, Andrew, Sam BOASE, Alkis PSALTIS and Peter-John WORMALD. Role of Bacterial and Fungal Biofilms in Chronic Rhinosinusitis. Current Allergy and Asthma Reports [online]. 2012, 12(2), 127-135 [cit. 2021-5-6]. ISSN 1529-7322. Doi:10.1007/s11882-012-0246-7

GALVEZ, Anita S., Angeles DURAN, Juan F. LINARES, et al. Protein Kinase Cζ Represses the Interleukin-6 Promoter and Impairs Tumorigenesis In Vivo. Molecular and Cellular Biology [online]. 2009, 29(1), 104-115 [cit. 2021-03-06]. ISSN 0270-7306. Doi:10.1128/MCB.01294-08

GARIĆ, Dušan, Juan B. DE SANCTIS, Juhi SHAH, Daciana Catalina DUMUT and Danuta RADZIOCH. Biochemistry of very-long-chain and long-chain ceramides in cystic fibrosis and other diseases: The importance of side chain. *Progress in Lipid Research* [online]. 2019, **74**, 130-144 [cit. 2021-03-22]. ISSN 01637827. Doi:10.1016/j.plipres.2019.03.001

GARIĆ, Dušan, Daciana Catalina DUMUT, Juhi SHAH, Juan Bautista DE SANCTIS and Danuta RADZIOCH. The role of essential fatty acids in cystic fibrosis and normalizing effect of fenretinide. Cellular and Molecular Life Sciences [online]. 2020, 77(21), 4255-4267 [cit. 2021-5-6]. ISSN 1420-682X. Doi:10.1007/s00018-020-03530-x

GASSERT, Evelyn, Elita AVOTA, Harry HARMS, Georg KROHNE, Erich GULBINS, Sibylle SCHNEIDER-SCHAULIES and Jae U. JUNG. Induction of Membrane Ceramides: A Novel Strategy to Interfere with T Lymphocyte Cytoskeletal Reorganisation in Viral Immunosuppression. *PLoS Pathogens* [online]. 2009, **5**(10) [cit. 2021-03-14]. ISSN 1553-7374. Doi:10.1371/journal.ppat.1000623

GLUCK, Louis, Marie V. KULOVICH, Robert C. BORER, Paul H. BRENNER, Gerald G. ANDERSON and William N. SPELLACY. Diagnosis of the respiratory distress syndrome by amniocentesis. American Journal of Obstetrics and Gynecology [online]. 1971, 109(3), 440-445 [cit. 2021-03-11]. ISSN 00029378. Doi:10.1016/0002-9378(71)90342-5

GRASSMÉ, Heike, Erich GULBINS, Birgit BRENNER, Klaus FERLINZ, Konrad SANDHOFF, Klaus HARZER, Florian LANG and Thomas F. MEYER. Acidic Sphingomyelinase Mediates Entry of N. gonorrhoeae into Nonphagocytic Cells. *Cell* [online]. 1997, **91**(5), 605-615 [cit. 2021-03-14]. ISSN 00928674. Doi:10.1016/S0092-8674(00)80448-1

GRASSME, H. CD95/CD95 Ligand Interactions on Epithelial Cells in Host Defense to Pseudomonas aeruginosa. *Science* [online]. 2000, **290**(5491), 527-530 [cit. 2021-03-14]. ISSN 00368075. Doi:10.1126/science.290.5491.527

GRASSMÉ, H., V. JENDROSSEK, A. RIEHLE, et al. Host defense against Pseudomonas aeruginosa requires ceramide-rich membrane rafts. *Nature Medicine* [online]. 2003A, **9**(3), 322-330 [cit. 2021-03-14]. ISSN 1078-8956. Doi:10.1038/nm823

GRASSMÉ, Heike, Aida CREMESTI, Richard KOLESNICK and Erich GULBINS. Ceramide-mediated clustering is required for CD95-DISC formation. *Oncogene* [online]. 2003B, **22**(35), 5457-5470 [cit. 2021-03-14]. ISSN 0950-9232. Doi:10.1038/sj.onc.1206540

GRASSMÉ, Heike, Andrea RIEHLE, Barbara WILKER and Erich GULBINS. Rhinoviruses Infect Human Epithelial Cells via Ceramide-enriched Membrane Platforms. *Journal of Biological Chemistry* [online]. 2005, **280**(28), 26256-26262 [cit. 2021-03-14]. ISSN 00219258. Doi:10.1074/jbc.M500835200

GROSS, Jürgen H. *Mass Spectrometry* [online]. Cham: Springer International Publishing, 2017 [cit. 2021-03-19]. ISBN 978-3-319-54397-0. Doi:10.1007/978-3-319-54398-7

GOLDKORN T, BALABAN N, SHANNON M, CHEA V, MATSUKUMA K, GILCHRIST D, WANG H, CHAN C. H_2O_2 acts on cellular membranes to generate ceramide signaling and initiate apoptosis in tracheobronchial epithelial cells. J Cell Sci. 1998 Nov;111 (Pt 21):3209-20. PMID: 9763515.

GOSEJACOB, Dominic, Philipp S. JÄGER, Katharina VOM DORP, et al. Ceramide Synthase 5 Is Essential to Maintain C16: 0-Ceramide Pools and Contributes to the Development of Diet-induced Obesity. Journal of Biological Chemistry [online]. 2016, 291(13), 6989-7003 [cit. 2021-03-07]. ISSN 00219258. Doi:10.1074/jbc.M115.691212

GUT, Ivo Glynne. DNA analysis by MALDI-TOF mass spectrometry. *Human Mutation* [online]. 2004, **23**(5), 437-441 [cit. 2021-03-17]. ISSN 1059-7794. Doi:10.1002/humu.20023

HANADA, Kentaro, Keigo KUMAGAI, Satoshi YASUDA, Yukiko MIURA, Miyuki KAWANO, Masayoshi FUKASAWA and Masahiro NISHIJIMA. Molecular machinery for non-vesicular trafficking of ceramide. *Nature* [online]. 2003, **426**(6968), 803-809 [cit. 2021-03-22]. ISSN 0028-0836. Doi:10.1038/nature02188

HANADA, Kentaro, Masahiro NISHIJIMA, Yuzuru AKAMATSU and Richard E. PAGANO. Both Sphingolipids and Cholesterol Participate in the Detergent Insolubility of Alkaline Phosphatase, a Glycosylphosphatidylinositol-anchored Protein, in Mammalian Membranes. *Journal of Biological Chemistry* [online]. 1995, **270**(11), 6254-6260 [cit. 2021-03-22]. ISSN 00219258. Doi:10.1074/jbc.270.11.6254

HARTMANN, Daniela, Jessica LUCKS, Sina FUCHS, et al. Long chain ceramides and very long chain ceramides have opposite effects on human breast and colon cancer cell growth. The International Journal of Biochemistry & Cell Biology [online]. 2012, 44(4), 620-628 [cit. 2021-03-04]. ISSN 13572725. Doi:10.1016/j.biocel.2011.12.019

HARVEY DJ. Matrix-assisted laser desorption/ionization mass spectrometry of carbohydrates. Mass Spectrom Rev. 1999 Nov-Dec;18(6):349-450. Doi: 10.1002/(SICI)1098-2787(1999)18:6<349::AID-MAS1>3.0.CO;2-H. PMID: 10639030.

HENRY, Brian, Regan ZIOBRO, Katrin Anne BECKER, Richard KOLESNICK and Erich GULBINS. Acid Sphingomyelinase. GULBINS, Erich a Irina PETRACHE, ed. *Sphingolipids: Basic Science and Drug Development* [online]. Vienna: Springer Vienna, 2013, 2013-3-9, s. 77-88 [cit. 2021-03-22]. Handbook of Experimental Pharmacology. ISBN 978-3-7091-1367-7. Doi:10.1007/978-3-7091-1368-4_4

IMGRUND, Silke, Dieter HARTMANN, Hany FARWANAH, et al. Adult Ceramide Synthase 2 (CERS2)-deficient Mice Exhibit Myelin Sheath Defects, Cerebellar Degeneration, and Hepatocarcinomas. *Journal of Biological Chemistry* [online]. 2009, **284**(48), 33549-33560 [cit. 2021-03-08]. ISSN 00219258. Doi:10.1074/jbc.M109.031971

ISHITSUKA, Yosuke and Dennis R. ROOP. Loricrin: Past, Present, and Future. *International Journal of Molecular Sciences* [online]. 2020, **21**(7) [cit. 2021-03-07]. ISSN 1422-0067. Doi:10.3390/ijms21072271

ISLAM, S.M. Anisul, Rekha PATEL and Mildred ACEVEDO-DUNCAN. Protein Kinase C-ζ stimulates colorectal cancer cell carcinogenesis via PKC-ζ/Rac1/Pak1/β-Catenin signaling cascade. *Biochimica et Biophysica Acta (BBA) - Molecular Cell Research* [online]. 2018, **1865**(4), 650-664 [cit. 2021-03-20]. ISSN 01674889. Doi:10.1016/j.bbamcr.2018.02.002

JENNEMANN, Richard, Mariona RABIONET, Karin GORGAS, et al. Loss of ceramide synthase 3 causes lethal skin barrier disruption. *Human Molecular Genetics* [online]. 2012, **21**(3), 586-608 [cit. 2021-03-07]. ISSN 1460-2083. Doi:10.1093/hmg/ddr494

KASAHARA, Yasunori, Rubin M. TUDER, Laimute TARASEVICIENE-STEWART, Timothy D. LE CRAS, Steven ABMAN, Peter K. HIRTH, Johannes WALTENBERGER and Norbert F. VOELKEL. Inhibition of VEGF receptors causes lung cell apoptosis and emphysema. *Journal of Clinical Investigation* [online]. 2000, **106**(11), 1311-1319 [cit. 2021-03-11]. ISSN 0021-9738. Doi:10.1172/JCI10259

KONO, Mari, Yide MI, Yujing LIU, Teiji SASAKI, Maria Laura ALLENDE, Yun-Ping WU, Tadashi YAMASHITA and Richard L. PROIA. The Sphingosine-1-phosphate Receptors S1P1, S1P2, and S1P3 Function Coordinately during Embryonic Angiogenesis. *Journal of Biological Chemistry* [online]. 2004, **279**(28), 29367-29373 [cit. 2021-03-22]. ISSN 00219258. Doi:10.1074/jbc.M403937200

KONSTANTINIDI, Efstathia M., Andreas S. LAPPAS, Anna S. TZORTZI a Panagiotis K. BEHRAKIS. Exhaled Breath Condensate: Technical and Diagnostic Aspects. *The Scientific World Journal* [online]. 2015,2015, 1-25 [cit. 2020-04-23]. DOI: 10.1155/2015/435160. ISSN 2356-6140.

KOWAL, Krzysztof, Ewa ŻEBROWSKA and Adrian CHABOWSKI. Altered Sphingolipid Metabolism Is Associated With Asthma Phenotype in House Dust Mite-Allergic Patients. *Allergy, Asthma & Immunology Research* [online]. 2019, **11**(3) [cit. 2021-03-01]. ISSN 2092-7355. Doi:10.4168/aair.2019.11.3.330

KOWALSKI, Michael P. and Gerald B. PIER. Localization of Cystic Fibrosis Transmembrane Conductance Regulator to Lipid Rafts of Epithelial Cells Is Required for Pseudomonas aeruginosa -Induced Cellular Activation. *The Journal of Immunology* [online]. 2003, **172**(1), 418-425 [cit. 2021-03-14]. ISSN 0022-1767. Doi:10.4049/jimmunol.172.1.418

KUMAGAI, Keigo, Satoshi YASUDA, Kazuo OKEMOTO, Masahiro NISHIJIMA, Shu KOBAYASHI, Kentaro HANADA. CERT Mediates Intermembrane Transfer of Various Molecular Species of Ceramides. *Journal of Biological Chemistry* [online]. 2005, **280**(8), 6488-6495 [cit. 2021-03-03]. ISSN 00219258. Doi:10.1074/jbc.M409290200

LAIKO, Victor V., Michael A. BALDWIN and Alma L. BURLINGAME. Atmospheric Pressure Matrix-Assisted Laser Desorption/Ionization Mass Spectrometry. *Analytical Chemistry* [online]. 2000, **72**(4), 652-657 [cit. 2021-03-18]. ISSN 0003-2700. Doi:10.1021/ac990998k

LAMOUR, Nadia F., Robert V. STAHELIN, Dayanjan S. WIJESINGHE, et al. Ceramide kinase uses ceramide provided by ceramide transport protein: localization to organelles of eicosanoid synthesis. *Journal of Lipid Research* [online]. 2007, **48**(6), 1293-1304 [cit. 2021-03-22]. ISSN 00222275. Doi:10.1194/jlr.M700083-JLR200

LAVIAD, Elad L., Samuel KELLY, Alfred H. MERRILL and Anthony H. FUTERMAN. Modulation of Ceramide Synthase Activity via Dimerization. *Journal of Biological Chemistry* [online]. 2012, **287**(25), 21025-21033 [cit. 2021-03-08]. ISSN 00219258. Doi:10.1074/jbc.M112.363580

LEVY, Michal, Elaine KHAN, Milo CAREAGA and Tzipora GOLDKORN. Neutral sphingomyelinase 2 is activated by cigarette smoke to augment ceramide-induced apoptosis in lung cell death. *American Journal of Physiology-Lung Cellular and Molecular Physiology* [online]. 2009, **297**(1), L125-L133 [cit. 2021-03-13]. ISSN 1040-0605. Doi:10.1152/ajplung.00031.2009

LINGWOOD, D. and K. SIMONS. Lipid Rafts As a Membrane-Organizing Principle. *Science* [online]. 2009, **327**(5961), 46-50 [cit. 2021-03-09]. ISSN 0036-8075. Doi:10.1126/science.1174621

LIU, Fangyu, Zhe ZHANG, László CSANÁDY, David C. GADSBY and Jue CHEN. Molecular Structure of the Human CFTR Ion Channel. *Cell* [online]. 2017, **169**(1), 85-95.e8 [cit. 2021-03-09]. ISSN 00928674. Doi:10.1016/j.cell.2017.02.024

LÖTVALL, Jan, Cezmi A. AKDIS, Leonard B. BACHARIER, et al. Asthma endotypes: A new approach to classification of disease entities within the asthma syndrome. *Journal of Allergy and Clinical Immunology* [online]. 2011, **127**(2), 355-360 [cit. 2021-03-10]. ISSN 00916749. Doi:10.1016/j.jaci.2010.11.037

McPHERSON, Christopher and Jennifer A. WAMBACH. Prevention and Treatment of Respiratory Distress Syndrome in Preterm Neonates. *Neonatal Network* [online]. 2018, **37**(3), 169-177 [cit. 2021-03-11]. ISSN 0730-0832. Doi:10.1891/0730-0832.37.3.169

MIZUTANI, Yukiko, Akio KIHARA and Yasuyuki IGARASHI. Mammalian Lass6 and its related family members regulate synthesis of specific ceramides. *Biochemical Journal* [online]. 2005, **390**(1), 263-271 [cit. 2021-03-07]. ISSN 0264-6021. Doi:10.1042/BJ20050291

MONTESANO, R., J. ROTH, A. ROBERT and L. ORCI. Non-coated membrane invaginations are involved in binding and internalization of cholera and tetanus toxins. *Nature* [online]. 1982, **296**(5858), 651-653 [cit. 2021-03-10]. ISSN 0028-0836. Doi:10.1038/296651a0

MUKHOPADHYAY, Archana, Sahar A. SADDOUGHI, Pengfei SONG, et al. Direct interaction between the inhibitor 2 and ceramide via sphingolipid-protein binding is involved in the regulation of protein phosphatase 2A activity and signaling. *The FASEB Journal* [online]. 2008, **23**(3), 751-763 [cit. 2021-03-05]. ISSN 0892-6638. Doi:10.1096/fj.08-120550

MUTLU, GÖKHAN M., KEVIN W. GAREY, RICHARD A. ROBBINS, LARRY H. DANZIGER a ISRAEL RUBINSTEIN. Collecti on and Analysis of Exhaled Breath Condensate in Humans. *American Journal of Respiratory and Critical Care Medicine* [online]. 2001,164(5), 731-737 [cit. 2020-04-23]. DOI: 10.1164/ajrccm.164.5.2101032. ISSN 1073-449X.

NICHOLS, Benjamin J., Anne K. KENWORTHY, Roman S. POLISHCHUK, Robert LODGE, Theresa H. ROBERTS, Koret HIRSCHBERG, Robert D. PHAIR and Jennifer LIPPINCOTT-SCHWARTZ. Rapid Cycling of Lipid Raft Markers between the Cell Surface and Golgi Complex. *Journal of Cell Biology* [online]. 2001, **153**(3), 529-542 [cit. 2021-03-10]. ISSN 0021-9525. Doi:10.1083/jcb.153.3.529

NURMINEN, Tuula A., Juha M. HOLOPAINEN, Hongxia ZHAO and Paavo K. J. KINNUNEN. Observation of Topical Catalysis by Sphingomyelinase Coupled To Microspheres. *Journal of the American Chemical Society* [online]. 2002, **124**(41), 12129-12134 [cit. 2021-03-13]. ISSN 0002-7863. Doi:10.1021/ja017807r

OSAWA, Yosuke, Hiroshi UCHINAMI, Jacek BIELAWSKI, Robert F. SCHWABE, Yusuf A. HANNUN a David A. BRENNER. Roles for C16-ceramide and Sphingosine 1-Phosphate in Regulating Hepatocyte Apoptosis in Response to Tumor Necrosis Factor-α. *Journal of Biological Chemistry* [online]. 2005, **280**(30), 27879-27887 [cit. 2021-03-04]. ISSN 00219258. Doi:10.1074/jbc.M503002200

PARTON, R. G., B. JOGGERST and K. SIMONS. Regulated internalization of caveolae. *Journal of Cell Biology* [online]. 1994, **127**(5), 1199-1215 [cit. 2021-03-20]. ISSN 0021-9525. Doi:10.1083/jcb.127.5.1199

PAUL, Arindam, Marsha DANLEY, Biswarup SAHA, Ossama TAWFIK and Soumen PAUL. PKCζ Promotes Breast Cancer Invasion by Regulating Expression of E-cadherin and Zonula Occludens-1 (ZO-1) via NFκB-p65. *Scientific Reports* [online]. 2015, **5**(1) [cit. 2021-03-06]. ISSN 2045-2322. Doi:10.1038/srep12520

PAUL, W., & STEINWEDEL, H. (1954). *U.S. Patent No. US2939952A*. Washington, DC: U.S. Patent and Trademark Office.

PELKMANS, Lucas a Ari HELENIUS. Endocytosis Via Caveolae. *Traffic* [online]. 2002, **3**(5), 311-320 [cit. 2021-03-22]. ISSN 13989219. Doi:10.1034/j.1600-0854.2002.30501.x

PETRACHE, Irina, Krzysztof KAMOCKI, Christophe POIRIER, et al. Ceramide Synthases Expression and Role of Ceramide Synthase-2 in the Lung: Insight from Human Lung Cells and Mouse Models. *PLoS ONE* [online]. 2013, **8**(5) [cit. 2021-03-08]. ISSN 1932-6203. Doi:10.1371/journal.pone.0062968

PETRACHE, Irina, Viswanathan NATARAJAN, Lijie ZHEN, et al. Ceramide upregulation causes pulmonary cell apoptosis and emphysema-like disease in mice. *Nature Medicine* [online]. 2005, **11**(5), 491-498 [cit. 2021-03-11]. ISSN 1078-8956. Doi:10.1038/nm1238

PEWZNER-JUNG, Yael, Ori BRENNER, Svantje BRAUN, et al. A Critical Role for Ceramide Synthase 2 in Liver Homeostasis. *Journal of Biological Chemistry* [online]. 2010, **285**(14), 10911-10923 [cit. 2021-03-08]. ISSN 00219258. Doi:10.1074/jbc.M109.077610

PEWZNER-JUNG, Yael, Shaghayegh TAVAKOLI TABAZAVAREH, Heike GRASSMÉ, et al. Sphingoid long chain bases prevent lung infection by Pseudomonas aeruginosa. *EMBO Molecular Medicine* [online]. 2014, **6**(9), 1205-1214 [cit. 2021-03-09]. ISSN 1757-4676. Doi:10.15252/emmm.201404075

PONIKAU, Jens U., David A. SHERRIS, Eugene B. KERN, Henry A. HOMBURGER, Evangelos FRIGAS, Thomas A. GAFFEY a Glenn D. ROBERTS. The Diagnosis and Incidence of Allergic Fungal Sinusitis. Mayo Clinic Proceedings [online]. 1999, 74(9), 877-884 [cit. 2021-5-6]. ISSN 00256196. Doi:10.4065/74.9.877

PULLMANNOVÁ, Petra, Ludmila PAVLÍKOVÁ, Andrej KOVÁČIK, et al. Permeability and microstructure of model stratum corneum lipid membranes containing ceramides with long (C16) and very long (C24) acyl chains. *Biophysical Chemistry* [online]. 2017, **224**, 20-31 [cit. 2021-03-20]. ISSN 03014622. Doi:10.1016/j.bpc.2017.03.004

PURI, Vishwajeet, Rikio WATANABE, Raman Deep SINGH, Michel DOMINGUEZ, Jennifer C. BROWN, Christine L. WHEATLEY, David L. MARKS and Richard E. PAGANO. Clathrin-dependent and independent internalization of plasma membrane sphingolipids initiates two Golgi targeting pathways. *Journal of Cell Biology* [online]. 2001, **154**(3), 535-548 [cit. 2021-03-10]. ISSN 1540-8140. Doi:10.1083/jcb.200102084

RABIONET, Mariona, Aline BAYERLE, Richard JENNEMANN, et al. Male meiotic cytokinesis requires ceramide synthase 3-dependent sphingolipids with unique membrane anchors. *Human Molecular Genetics* [online]. 2015, **24**(17), 4792-4808 [cit. 2021-03-07]. ISSN 0964-6906. Doi:10.1093/hmg/ddv204

RIORDAN, J. ROMMENS, B KEREM, et al. Identification of the cystic fibrosis gene: cloning and characterization of complementary DNA. *Science* [online]. 1989, **245**(4922), 1066-1073 [cit. 2021-03-09]. ISSN 0036-8075. Doi:10.1126/science.2475911

ROTHBERG, K. G., Y. S. YING, J. F. KOLHOUSE, B. A. KAMEN and R. G. ANDERSON. The glycophospholipid-linked folate receptor internalizes folate without entering the clathrin-coated pit endocytic pathway. *Journal of Cell Biology* [online]. 1990, **110**(3), 637-649 [cit. 2021-03-20]. ISSN 0021-9525. Doi:10.1083/jcb.110.3.637

ROTHBERG, Karen G., John E. HEUSER, William C. DONZELL, Yun-Shu YING, John R. GLENNEY and Richard G.W. ANDERSON. Caveolin, a protein component of caveolae membrane coats. *Cell* [online]. 1992, **68**(4), 673-682 [cit. 2021-03-10]. ISSN 00928674. Doi:10.1016/0092-8674(92)90143-Z

SADDOUGHI, Sahar A., Salih GENCER, Yuri K. PETERSON, et al. Sphingosine analogue drug FTY720 targets I2PP2A/SET and mediates lung tumour suppression via activation of PP2A-RIPK1-dependent necroptosis. *EMBO Molecular Medicine* [online]. 2013, **5**(1), 105-121 [cit. 2021-03-05]. ISSN 1757-4676. Doi:10.1002/emmm.201201283

SAHARA, Setsuko, Mamoru AOTO, Yutaka EGUCHI, Naoko IMAMOTO, Yoshihiro YONEDA and Yoshihide TSUJIMOTO. Acinus is a caspase-3-activated protein required for apoptotic chromatin condensation. *Nature* [online]. 1999, **401**(6749), 168-173 [cit. 2021-03-13]. ISSN 0028-0836. Doi:10.1038/43678

SAKABE, Jun-ichi, Mami YAMAMOTO, Satoshi HIRAKAWA, et al. Kallikrein-related Peptidase 5 Functions in Proteolytic Processing of Profilaggrin in Cultured Human Keratinocytes. *Journal of Biological Chemistry* [online]. 2013, **288**(24), 17179-17189 [cit. 2021-03-07]. ISSN 00219258. Doi:10.1074/jbc.M113.476820

SCHNITZER, J. E., P. OH, E. PINNEY and J. ALLARD. Filipin-sensitive caveolae-mediated transport in endothelium: reduced transcytosis, scavenger endocytosis, and capillary permeability of select macromolecules. *Journal of Cell Biology* [online]. 1994, **127**(5), 1217-1232 [cit. 2021-03-10]. ISSN 0021-9525. Doi:10.1083/jcb.127.5.1217

SCHUCK, S., M. HONSHO, K. EKROOS, A. SHEVCHENKO and K. SIMONS. Resistance of cell membranes to different detergents. *Proceedings of the National Academy of Sciences* [online]. 2003, **100**(10), 5795-5800 [cit. 2021-03-22]. ISSN 0027-8424. Doi:10.1073/pnas.0631579100

SEBBAGH, Michaël, Claire RENVOIZÉ, Jocelyne HAMELIN, Nicole RICHÉ, Jacques BERTOGLIO and Jacqueline BRÉARD. Caspase-3-mediated cleavage of ROCK I induces MLC phosphorylation and apoptotic membrane blebbing. *Nature Cell Biology* [online]. 2001, **3**(4), 346-352 [cit. 2021-03-13]. ISSN 1465-7392. Doi:10.1038/35070019

SEITZ, Aaron P., Heike GRASSMÉ, Michael J. EDWARDS, Yael PEWZNER-JUNG and Erich GULBINS. Ceramide and sphingosine in pulmonary infections. *Biological Chemistry* [online]. 2015, **396**(6-7), 611-620 [cit. 2021-03-13]. ISSN 1437-4315. Doi:10.1515/hsz-2014-0285

SIMANSHU, Dhirendra K., Ravi Kanth KAMLEKAR, Dayanjan S. WIJESINGHE, et al. Non-vesicular trafficking by a ceramide-1-phosphate transfer protein regulates eicosanoids. *Nature* [online]. 2013, **500**(7463), 463-467 [cit. 2021-03-22]. ISSN 0028-0836. Doi:10.1038/nature12332

SIMONIS, Alexander, Sabrina HEBLING, Erich GULBINS, Sibylle SCHNEIDER-SCHAULIES, Alexandra SCHUBERT-UNKMEIR and Christoph TANG. Differential Activation of Acid Sphingomyelinase and Ceramide Release Determines Invasiveness of Neisseria meningitidis into Brain Endothelial Cells. *PLoS Pathogens* [online]. 2014, **10**(6) [cit. 2021-03-14]. ISSN 1553-7374. Doi:10.1371/journal.ppat.1004160

SKIBBENS, J. E., M. G. ROTH and K. S. MATLIN. Differential extractability of influenza virus hemagglutinin during intracellular transport in polarized epithelial cells and nonpolar fibroblasts. *Journal of Cell Biology* [online]. 1989, **108**(3), 821-832 [cit. 2021-03-20]. ISSN 0021-9525. Doi: 10.1083/jcb.108.3.821

SNIDER, GL; KLEINERMAN, J; THURLBECK, WM; BENGALI, ZH. The definition of emphysema: Report of a National Heart, Lung, and Blood Institute, Division of Lung Diseases workshop. American Review of Respiratory Disease. 1985. [cit. 2021-03-07]. ISSN: 0003-0805

SISKIND Leah J., Richard N. KOLESNICK and Marco COLOMBINI. Ceramide Channels Increase the Permeability of the Mitochondrial Outer Membrane to Small Proteins. *Journal of Biological Chemistry* [online]. 2002, **277**(30), 26796-26803 [cit. 2021-03-04]. ISSN 00219258. Doi:10.1074/jbc.M200754200

SPENCER, Charlotte A. a Mark GROUDINE. *Control of c-myc Regulation in Normal and Neoplastic Cells* [online]. *Advances in Cancer Research,* 1991 1-48 [cit. 2021-03-20]. ISBN 9780120066568. Doi:10.1016/S0065-230X(08)60476-5

SRIBNEY, Michael. Enzymatic synthesis of ceramide. *Biochimica et Biophysica Acta (BBA) - Lipids and Lipid Metabolism* [online]. 1966, **125**(3), 542-547 [cit. 2021-03-20]. ISSN 00052760. Doi:10.1016/0005-2760(66)90042-7

STAMMBERGER, H., R. JAKSE a F. BEAUFORT. Aspergillosis of the Paranasal Sinuses. Annals of Otology, Rhinology & Laryngology [online]. 2016, 93(3), 251-256 [cit. 2021-5-6]. ISSN 0003-4894. Doi:10.1177/000348948409300313

STEINERT, P. M., J. S. CANTIERI, D. C. TELLER, J. D. LONSDALE-ECCLES and B. A. DALE. Characterization of a class of cationic proteins that specifically interact with intermediate filaments. *Proceedings of the National Academy of Sciences* [online]. 1981, **78**(7), 4097-4101 [cit. 2021-03-07]. ISSN 0027-8424. Doi:10.1073/pnas.78.7.4097

STIBAN, Johnny and Meenu PERERA. Very long chain ceramides interfere with C16-ceramide-induced channel formation: A plausible mechanism for regulating the initiation of intrinsic apoptosis. *Biochimica et Biophysica Acta (BBA) - Biomembranes* [online]. 2015, **1848**(2), 561-567 [cit. 2021-03-20]. ISSN 00052736. Doi:10.1016/j.bbamem.2014.11.018

STOFFEL, Wilhelm, Guido STICHT and Dac LEKIM. Metabolism of Sphingosine Bases, IX. Degradation in vitro of Dihydrosphingosine and Dihydrosphingosine phosphate to Palmitaldehyde and Ethanolamine phosphate. *Hoppe-Seyler´s Zeitschrift für physiologische Chemie* [online]. 1968, **349**(2), 1745-1748 [cit. 2021-03-14]. ISSN 0018-4888. Doi:10.1515/bchm2.1968.349.2.1745

SUZUKI, Atsushi, Tomoyuki YAMANAKA, Tomonori HIROSE, et al. Atypical Protein Kinase C Is Involved in the Evolutionarily Conserved Par Protein Complex and Plays a Critical Role in Establishing Epithelia-Specific Junctional Structures. *Journal of Cell Biology* [online]. 2001, **152**(6), 1183-1196 [cit. 2021-03-20]. ISSN 0021-9525. Doi:10.1083/jcb.152.6.1183

THOMAS, Rexford L., Christopher M. MATSKO, Michael T. LOTZE and Andrew A. AMOSCATO. Mass Spectrometric Identification of Increased C16 Ceramide Levels During Apoptosis. *Journal of Biological Chemistry* [online]. 1999, **274**(43), 30580-30588 [cit. 2021-03-04]. ISSN 00219258. Doi:10.1074/jbc.274.43.30580

TURNER, S., S. C. COTTON, C. D. EMELE, et al. Reducing Asthma Attacks in Children using Exhaled Nitric Oxide as a biomarker to inform treatment strategy: a randomised trial (RAACENO). Trials [online]. 2019, 20(1) [cit. 2021-5-6]. ISSN 1745-6215. Doi:10.1186/s13063-019-3500-7

TURPIN, Sarah M., Hayley T. NICHOLLS, Diana M. WILLMES, et al. Obesity-Induced CerS6-Dependent C16: 0 Ceramide Production Promotes Weight Gain and Glucose Intolerance. *Cell Metabolism* [online]. 2014, **20**(4), 678-686 [cit. 2021-03-08]. ISSN 15504131. Doi:10.1016/j.cmet.2014.08.002

UTERMÖHLEN, Olaf, Jasmin HERZ, Michael SCHRAMM and Martin KRÖNKE. Fusogenicity of membranes: The impact of acid sphingomyelinase on innate immune responses. *Immunobiology* [online]. 2008, **213**(3-4), 307-314 [cit. 2021-03-21]. ISSN 01712985. Doi:10.1016/j.imbio.2007.10.016

WALLACE, M. Ariel Geer a Joachim D. PLEIL. Evolution of clinical and environmental health applications of exhaled breath research: Review of methods and instrumentation for gas-phase, condensate, and aerosols. *Analytica Chimica Acta* [online]. 2018, 1024, 18-38 [cit. 2020-04-23]. DOI: 10.1016/j.aca.2018.01.069. ISSN 00032670

YANG, Yang and Stefan UHLIG. The role of sphingolipids in respiratory disease. *Therapeutic Advances in Respiratory Disease* [online]. 2011, **5**(5), 325-344 [cit. 2021-03-01]. ISSN 1753-4658. Doi:10.1177/1753465811406772

YAVIN, Ephraim; GATT, Shimon (1969). *Enzymic hydrolysis of sphingolipids. VIII. Purification and properties of rat brain ceramidase. Biochemistry, 8(4), 1692–1698.* [cit. 2021-03-01]. Doi:10.1021/bi00832a052

YEH, Elizabeth, Melissa CUNNINGHAM, Hugh ARNOLD, et al. A signalling pathway controlling c-Myc degradation that impacts oncogenic transformation of human cells. Nature Cell Biology [online]. 2004, 6(4), 308-318 [cit. 2021-03-05]. ISSN 1465-7392. Doi:10.1038/ncb1110

YOON, Hyoung Kyu, Yong-Bum PARK, Chin Kook RHEE, Jin Hwa LEE and Yeon-Mok OH. Summary of the Chronic Obstructive Pulmonary Disease Clinical Practice Guideline Revised in 2014 by the Korean Academy of Tuberculosis and Respiratory Disease. *Tuberculosis and Respiratory Diseases* [online]. 2017, **80**(3) [cit. 2021-03-10]. ISSN 1738-3536. Doi:10.4046/trd.2017.80.3.230

ZHANG, Yang, Xiang LI, Alexander CARPINTEIRO and Erich GULBINS. Acid Sphingomyelinase Amplifies Redox Signaling in Pseudomonas aeruginosa -Induced

Macrophage Apoptosis. *The Journal of Immunology* [online]. 2008, **181**(6), 4247-4254 [cit. 2021-03-14]. ISSN 0022-1767. Doi:10.4049/jimmunol.181.6.4247

ZHANG, Yang, Xiang LI, Heike GRASSMÉ, Gerd DÖRING a Erich GULBINS. Alterations in Ceramide Concentration and pH Determine the Release of Reactive Oxygen Species by Cftr -Deficient Macrophages on Infection. *The Journal of Immunology* [online]. 2010, **184**(9), 5104-5111 [cit. 2021-03-14]. ISSN 0022-1767. Doi:10.4049/jimmunol.0902851

ZHAO, Lihong, Stefka D. SPASSIEVA, Thomas J. JUCIUS, et al. A Deficiency of Ceramide Biosynthesis Causes Cerebellar Purkinje Cell Neurodegeneration and Lipofuscin Accumulation. *PLoS Genetics* [online]. 2011, **7**(5) [cit. 2021-03-07]. ISSN 1553-7404. Doi:10.1371/journal.pgen.1002063

9 APPENDIX

Graph 7 – Standard curve for ceramide C14

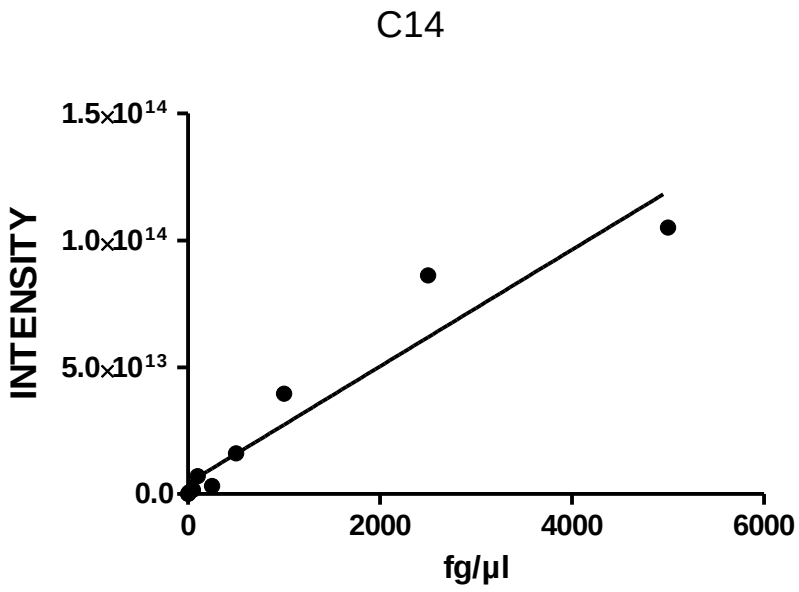

Graph 8 – Standard curve for ceramide C16

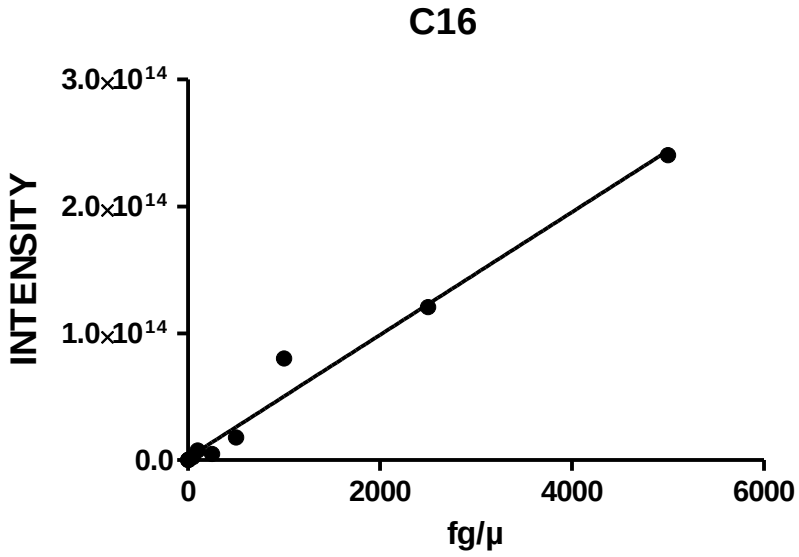

Graph 9 – Standard curve for ceramide C17

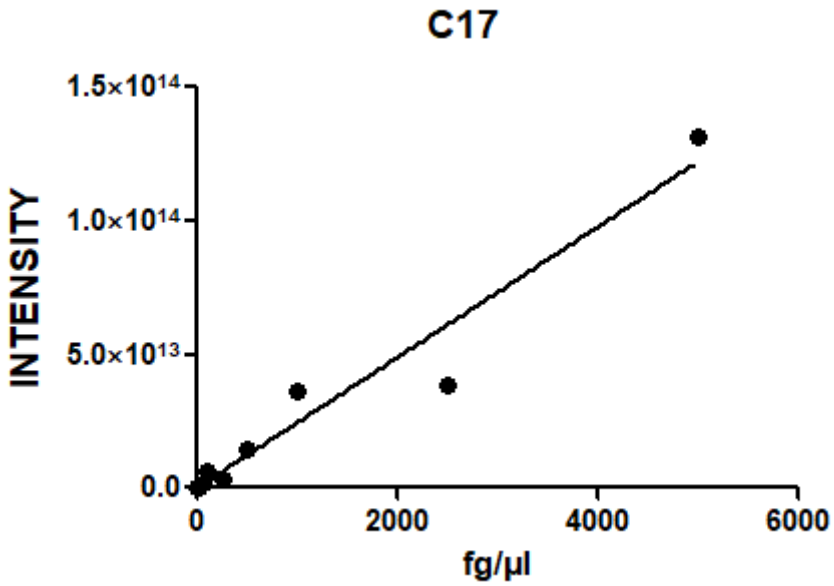

Graph 10 – Standard curve for ceramide C18

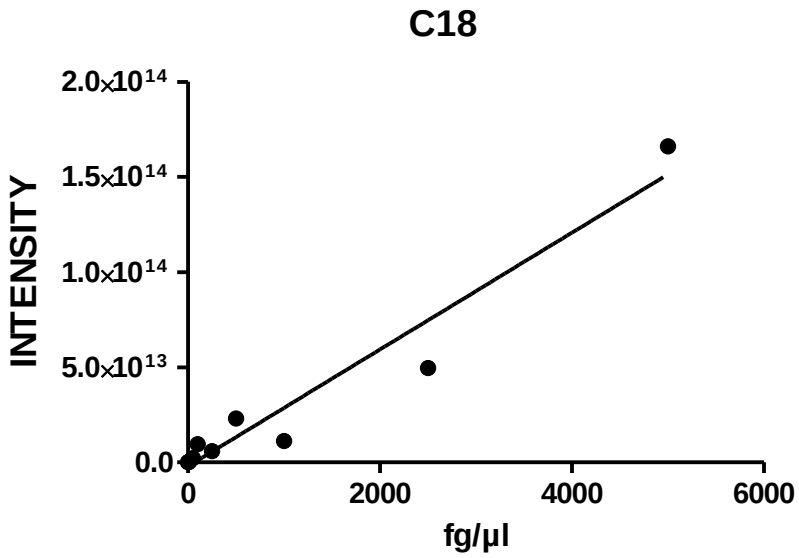

Graph 11 – Standard curve for ceramide C18:1

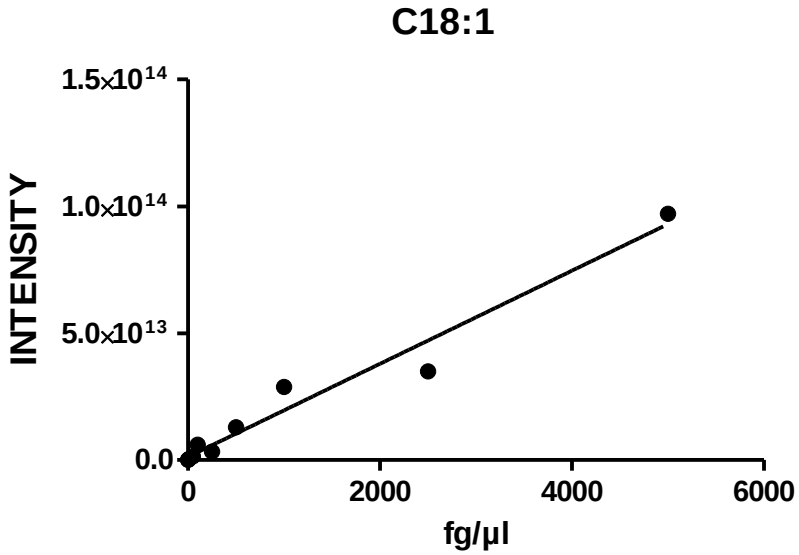

Graph 12 – Standard curve for ceramide C20

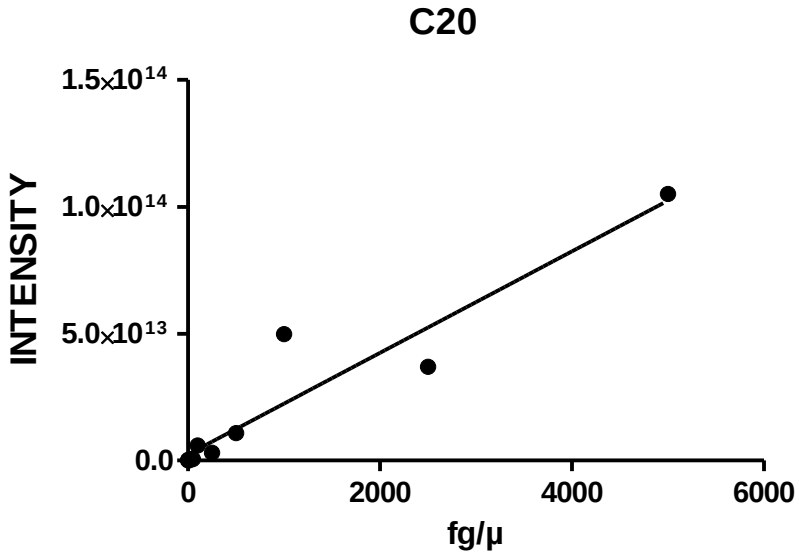

Graph 13 – Standard curve for ceramide C22

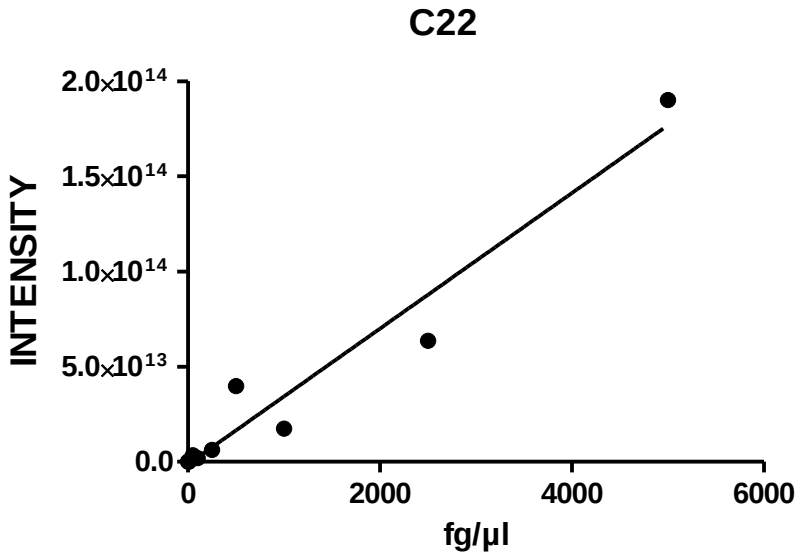

Graph 14 – Standard curve for ceramide C24

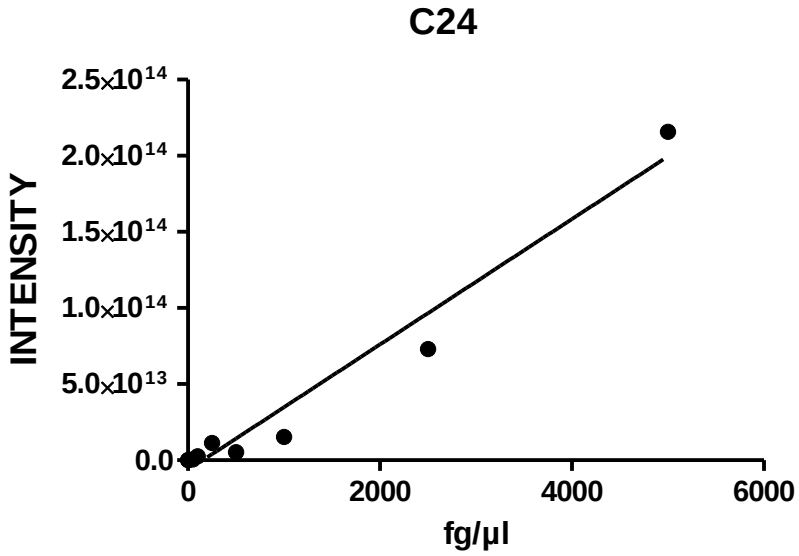

Graph 15 – Standard curve for ceramide C24:1

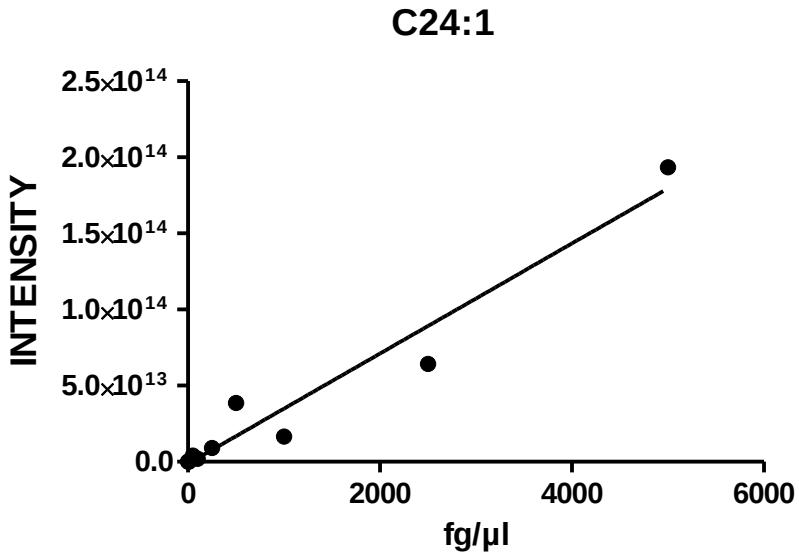

Graph 16 – Standard curve for ceramide C26

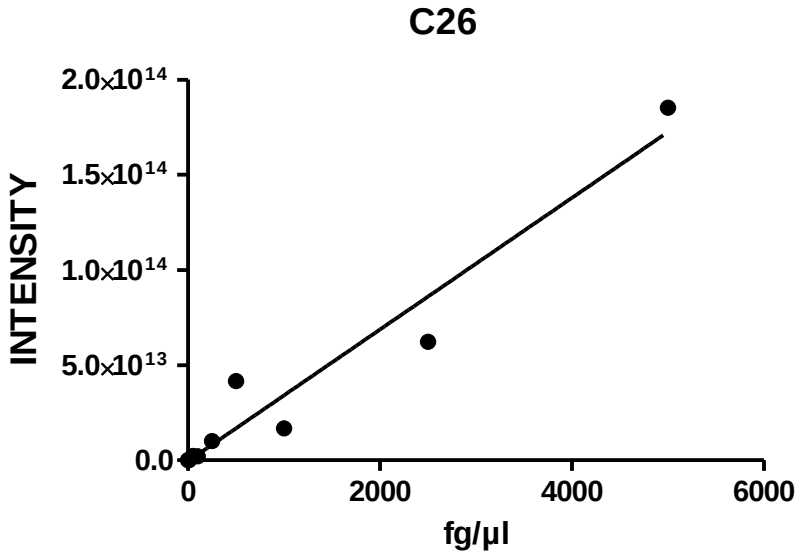

Graph 17 – Standard curve for ergosterol